

AD 679588

# *Aerospace Research Center*

## LIQUID LASER PARAMETERS

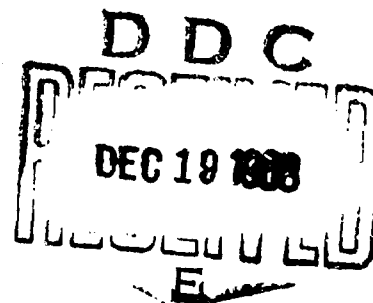
Contract NOmr -4644(00)

### FINAL REPORT

Prepared for  
PHYSICAL SCIENCES DIVISION  
OFFICE OF NAVAL RESEARCH  
WASHINGTON, D.C.

November 25, 1968

AEROSPACE RESEARCH CENTER  
SINGER-GENERAL PRECISION, INC.  
KEARFOTT GROUP  
LITTLE FALLS, NEW JERSEY



This document has been approved  
for public release and sale; its  
distribution is unlimited.

MATERIALS DEPARTMENT

LIQUID LASER PARAMETERS

Contract NO. ~~4644~~ 4644(C)  
FINAL REPORT

by

Mr. William Block  
Dr. Robert Barnes  
and  
Dr. Daniel Grafstein

This Research is Part of Project DEFENDER  
Sponsored by the  
Advanced Research Projects Agency  
Department of Defense  
APRA Order No. 306-62  
Project Code No. 4730

November 25, 1968

AEROSPACE RESEARCH CENTER  
SINGER-GENERAL PRECISION, INC.  
KEARFOTT GROUP  
LITTLE FALLS, NEW JERSEY

### ADMINISTRATIVE INFORMATION

This is the Final Report on the program entitled Liquid Laser Parameters which covers research done under Contract NONr-4644(00) between the Office of Naval Research and the Aerospace Research Center of Singer-General Precision, Inc., Little Falls, New Jersey. This research was part of Project DEFENDER sponsored by the Advanced Research Projects Agency, Department of Defense, ARPA Order No. 306-62 Project Code No. 4730. The work was administered by the Scientific Officer, Physical Sciences Division, Office of Naval Research, Code 421, Mr. F. B. Isakson. Dr. Irving Rowe of the Office of Naval Research, New York, has acted as Project Engineer. This report covers research performed during the period August 1, 1964 to July 31, 1968.

The Project Supervisor at the Aerospace Research Center was Dr. Daniel Grafstein, Manager of the Materials Department. Contributors over the course of this program were Dr. Robert Barnes, Mr. William Block, Dr. Norman Blumenthal, Dr. Raymond Borkowski, Mr. Alfred Brauer, Dr. Cecil Ellis, Dr. Harvey Forest, Dr. Aryeh Samuel and Dr. David Williams.

### SUMMARY

This program was designed to study the influence of chemical and physical environmental factors upon the intensity, efficiency and lifetimes of rare earth phosphorescence in liquid systems. The objective was the development of criteria for the selection of optimum coordinating ligands, counter ions and solvents for rare earths so that useful and efficient high power solution lasers could be developed. The ultimate goal of this research was the development of a candidate liquid that could be used in a circulating laser system.

As shown in the following sections a large number of rare earth coordination compounds were synthesized and studied both in the solid state and in solution. A considerable amount of information relating fluorescence to chemical structure and environment was accumulated. (1,2,3) These results led us, in the final phase of the program, to demonstrations of lasing in solutions of neodymium (III) in the solvent mixture phosphorus oxychloride-tin tetrachloride. (4)

From our earlier work during this program it was concluded that several environmental factors were important in influencing rare earth fluorescence.

1. Light atoms such as hydrogen and deuterium which would contribute to high-energy vibrational frequencies must be removed from the immediate ligand field surrounding the rare earth ion.
2. Vibrational frequencies in the ligand or coordinating solvent should closely match the energy gaps between the initially excited optically pumped level and the emitting level in order to efficiently populate that level by a cascade process. These same vibrational frequencies, however, must be sufficiently different from the frequency of lasing radiation so as not to promote non-radiative transitions from the emitting level.
3. The solvent must be transparent in the optical regions available for direct pumping of the rare earth and in the optical region of the phosphorescence wavelengths of the rare earth. Also, the solvent can play an important role in enhancing the absorption bands of the rare earth ion.

4. The solvent must possess a sufficiently high dielectric constant in order to dissolve the ionic rare earth coordination complexes. A wide liquid range, low vapor pressure and a low viscosity is required to enable a laser to be operated without undue restrictions such as heating or cooling.

Of the several organic and inorganic solvents that were investigated, those in which a phosphorus-oxygen linkage was coordinated to the rare earth appeared most promising. A significant enhancement in europium phosphorescence was observed when europium salts were dissolved in triethyl phosphate, tributyl phosphate and hexamethylphosphoramide. In addition, a variation in selectivity of particular emission bands was observed; this selectivity depended on the structure and symmetry of the ligand field. Of the P-O containing ligands which were investigated, phosphorus oxychloride was of particular interest because the phosphorescent spectrum of the solid complex  $\text{EuCl}_3 \cdot \text{XPOCl}_3$  consisted almost entirely of the  $^5\text{D}_0 \rightarrow ^7\text{F}_2$  transition. Because of this selectivity and the absence of hydrogen atoms which would contribute to high-energy vibrational frequencies, phosphorus oxychloride was one of the first solvents chosen for a limited attempt to demonstrate lasing.

Neodymium was the rare earth of choice because of certain energy considerations and because it is one of the best performing laser active rare earth ions. Information was already available on the somewhat similar selenium oxychloride laser<sup>(5)</sup>. The maximum fundamental vibrational frequency in phosphorus oxychloride is at  $1285 \text{ cm}^{-1}$  (assigned to the P-O stretch) which is considerably smaller than that for the lasing transition from the  $^4\text{F}_{3/2}$  level to the  $^4\text{I}_{11/2}$  level - about  $9400 \text{ cm}^{-1}$  and also for the smallest energy transition from the  $^4\text{F}_{3/2}$  level - that of  $^4\text{F}_{3/2} \rightarrow ^4\text{I}_{15/2}$  at  $5500 \text{ cm}^{-1}$ . Non-radiative transfer of energy from the  $^4\text{F}_{3/2}$  lasing emitting level should be minimized.

We consider it useful to summarize the properties of the neodymium, (III)  $\text{POCl}_3\text{-SnCl}_4$  system. Although neodymium oxide is not appreciably soluble in phosphorus oxychloride, addition of  $\text{SnCl}_4$  brings the oxide into solution. Dilute solutions of  $\text{Nd}^{3+}$  up to 1.2% Nd by weight were easily prepared in the solvent mixture  $\text{POCl}_3\text{-SnCl}_4$  using conventional laboratory procedures and taking only ordinary care to prevent contamination by

atmospheric moisture. These solutions are very stable and have a viscosity about that of water (1 cp) at room temperature. The  $1.06\mu$  neodymium phosphorescence from the solution is very intense (Figure 5) and the visible absorption spectrum (Figure 6) is similar to that expected for a neodymium containing solution. Lasing in this  $\text{Nd}^{3+}$  -  $\text{POCl}_3$ - $\text{SnCl}_4$  solution was first demonstrated in a quartz cell having a 12 mm bore and 12.5 cm path length with plane parallel silica plates on the ends. The cell was designed to occupy the same volume in a commercial Korad laser head that was normally occupied by a ruby rod. External flat mirrors, one with a 90% reflective coating and the other with a totally reflecting dielectric coating completed the cavity. Pulsed excitation was accomplished through an unfiltered Korad helical air-cooled xenon flash lamp. Random spiking with very large intensity increase over the fluorescence level at  $1.06\mu$  and ringing effects are illustrated in Figures 7-11. For a 1.2% by weight solution of  $\text{Nd}^{3+}$  in  $\text{POCl}_3$ - $\text{SnCl}_4$  (0.15 N in  $\text{Nd}^{3+}$ ) the input threshold was found to be 1300 J. This compares with a value of 1100 J for a four inch long, 3/8" diameter, 5%-neodymium-doped glass rod in the same cavity. Lower thresholds could probably be obtained with a better designed cavity. The solution is quite stable in a closed system and does not exhibit any visual decomposition phenomenon. Further work must be carried out on optimization of its lasing properties, particularly with respect to an optimum neodymium concentration and ratio of phosphorus to tin as well as circulation of the media.

TABLE OF CONTENTS

	<u>Page</u>
ADMINISTRATIVE INFORMATION	i
SUMMARY	ii
LIST OF TABLES	vii
LIST OF FIGURES	viii
LIST OF PUBLICATIONS	ix
I. INTRODUCTION	1
II. DISCUSSION	3
A. The Neodymium (III) Phosphorus Oxychloride - Tin Tetrachloride Laser	3
B. Effect of Chemical Environment on Phosphorescence	7
1. Comparison of Phosphorescent Output of Rare Earths in H <sub>2</sub> O Versus D <sub>2</sub> O	7
a. EuCl <sub>3</sub>	7
b. SmCl <sub>3</sub>	21
c. TbCl <sub>3</sub>	22
2. Comparison of the Phosphorescent Output of Europium in CH <sub>3</sub> OH, CH <sub>3</sub> OD and CD <sub>3</sub> OH	23
3. Phosphorescence of Europium (III) Complexes with P-O Containing Ligands	25
a. EuCl <sub>3</sub> · 3 [ O = P(OR) <sub>3</sub> ]	25
b. Eu[ O <sub>2</sub> P(OR) <sub>2</sub> ] <sub>3</sub>	28
c. EuCl <sub>3</sub> - 3 Hexamethylphosphoramide	31
d. EuCl <sub>3</sub> · XPOCl <sub>3</sub>	32
e. Quantum Efficiency Measurements of Eu <sup>+3</sup> - TEP Solutions	34
4. Complexes of Rare Earths with Dimethylacetamide and its Homologs	36
a. Preparation and Characterization of Complexes of Eu <sup>+3</sup> , Tb <sup>+3</sup> and Nd <sup>+3</sup>	36
b. Phosphorescence of Complexes of Eu <sup>+3</sup> with Dimethylacetamide and its Homologs	39
c. Phosphorescence of the Tb <sup>+3</sup> - Dimethylacetamide Complex	41
d. Phosphorescent Fine Structure of Complexes of Tb <sup>+3</sup> and Eu <sup>+3</sup> with Dimethylacetamide	43
e. Phosphorescence of the Nd <sup>+3</sup> - Dimethylacetamide Complex	44

AEROSPACE RESEARCH CENTER • SINGER GENERAL PRECISION, INC.

Table of Contents (cont'd)

5. Criteria for Pumping Europium Systems	<u>Page</u> 46
6. Power Threshold Calculation for Europium Systems	50
7. Phosphorescent Intensities and Lifetimes of $Tb^{+3}$ Complexes	55
8. Phosphorescence of Complexes of Samarium (III) and Dysprosium (III) with Triethyl Phosphate	59
III. RECOMMENDATIONS	60
REFERENCES	61
APPENDIX	A-i
DISTRIBUTION LIST	62



LIST OF TABLES

<u>Table</u>		<u>Page</u>
1	Phosphorescence of $\text{EuCl}_3$ in $\text{H}_2\text{O}$ and in $\text{D}_2\text{O}$	20
2	Phosphorescence of $\text{SmCl}_3$ in $\text{H}_2\text{O}$ and in $\text{D}_2\text{O}$	21
3	Phosphorescence of $\text{TbCl}_3$ in $\text{H}_2\text{O}$ and in $\text{D}_2\text{O}$	22
4	Phosphorescence of Europium in Methanol and Its Deuterium Substituted Derivatives	24
5	Effect of Solvent on the Phosphorescence of $\text{EuCl}_3 \cdot 3\text{HMPA}$	33
6	Elemental Analyses of DMAC Complexes	37
7	Phosphorescent Intensities of Complexes of DMAC and Its Homologs with Europium (III)	40
8	Relative Phosphorescent Intensities of Neodymium and Terbium in Different Solvents	42
9	Phosphorescent Fine Structure of Europium and Terbium in DMAC and Water Systems	45
10	Relative Phosphorescent Intensities of Terbium Lines	54
11	Lifetimes of Various $\text{Tb}^{+3}$ Complexes	55

LIST OF FIGURES

<u>Figure</u>		<u>Page</u>
1	Energy Level Diagram for Trivalent Nd, Eu and Tb.	8
2	Absorption Spectrum of Phosphorus Oxychloride	9
3	Absorption Spectrum of Stannic Chloride	10
4	Absorption Spectrum of 5:1 Volume Ratio of $\text{POCl}_3$ to $\text{SnCl}_4$	11
5	Phosphorescence Spectrum of a Solution of $\text{Nd}_2\text{O}_3$ (0.075 Molar) in the Solvent System, $\text{POCl}_3 - \text{SnCl}_4$	12
6	Absorption Spectrum of a Solution of $\text{Nd}_2\text{O}_3$ (0.075 Molar) in the Solvent System, $\text{POCl}_3 - \text{SnCl}_4$	13
7	$\text{Nd}_2\text{O}_3 - \text{POCl}_3 - \text{SnCl}_4$ ; Incipient Spiking at 1060 nm Just Above Threshold	14
8	$\text{Nd}_2\text{O}_3 - \text{POCl}_3 - \text{SnCl}_4$ ; Random Spiking at 1060 nm, 380 Percent Above Threshold	15
9	$\text{Nd}_2\text{O}_3 - \text{POCl}_3 - \text{SnCl}_4$ ; Limit Cycle Behavior at 1060 nm, Input: 3000J	16
10	$\text{Nd}_2\text{O}_3 - \text{POCl}_3 - \text{SnCl}_4$ ; Limit Cycle Behavior at 1060 nm, Input: 5000J	17
11	$\text{Nd}_2\text{O}_3 - \text{POCl}_3 - \text{SnCl}_4$ ; Limit Cycle Behavior at 1060 nm, Expanded Time Scale, Input: 5000J	18
12	Direct Photograph of the Laser Beam Showing Beam Collimation	19
13	Phosphorescence of Europium Chloride in Tributylphosphate	26
14	Phosphorescence of Europium Chloride in Triethylphosphate	27
15	Phosphorescence of $\text{Eu}[\text{O}_2\text{P}(\text{OC}_2\text{H}_5)_2]_3$	29
16	Phosphorescence of $\text{Eu}[\text{O}_2\text{P}(\text{OC}_4\text{H}_9)_2]_3$	30
17	Energy Level Diagram of $\text{Eu}^{+3}$	48
18	$4F^8$ Energy Level Diagram for $\text{Tb}^{+3}$	58

LIST OF PUBLICATIONS

This program has contributed, in all or part, to the following papers.

1. "Selected Enhancement of Fluorescence from Some Rare-Earth Salts in Solution", R. P. Borkowski, H. Forest and D. Grafstein, J. Chem. Phys., 42, 2974 (1965).
2. "Enhancement of  $\text{Eu}^{3+}$  Fluorescence by Complex Formation", H. Forest, A. Samuel and D. Grafstein, J. Opt. Soc. Amer., 56, 548 (1966).
3. "New Room Temperature Liquid Laser:  $\text{Nd(III)}$  in  $\text{POCl}_3 - \text{SnCl}_4$ ", N. Blumenthan, C. Ellis and D. Grafstein, J. Chem. Phys., 48, 5726 (1968).

## I. INTRODUCTION

The fluorescence, phosphorescence and absorption characteristics of rare earth ions in solution are of great interest in the development of liquid laser systems. The chosen liquids serve not only as mobile media to dissolve the metal salt but also to precisely control the immediate chemical environments around each rare earth ion and thereby favorably influence phosphorescence and other properties relevant to laser activity. The objective of the work reported herein was to develop criteria for the selection of optimum rare earth solutes and solvents so that useful and efficient high-power circulating liquid lasers could be developed. Most laser media are gaseous or solid and a considerable research effort has already resulted in improved performance and high power from such lasers. However, comparatively little effort has been expended in the use of a liquid as the active medium for a laser. Solid lasers have several deficiencies that could be overcome by the use of liquid systems. A high degree of optical perfection is difficult to attain in crystals and glasses. These often contain imperfections as a result of the fabricating process. Liquids are not subject to such defects. Although liquids do have significant changes in the index of refraction with changes in temperature, this defect could be minimized by circulation. High power solid lasers tend to craze and crack, a problem that would not be encountered with a liquid system since liquids tend to be self-healing. In addition, the cost of an optically perfect rod is quite high whereas the cost of chemicals for a liquid system would be low.

At the time this program was initiated, only tetrakis europium(III) B-diketonate type chelates had been shown to be capable of laser action in acetonitrile or methanol-ethanol solutions. <sup>(6,7)</sup> Direct excitation of europium(III) had previously been shown to be quite difficult because the absorption bands in this ion are weak. The function of the ligand in the chelate is to absorb a large amount of the pump flux and efficiently transfer the energy to the europium(III) electronic system which then phosphoresces in its characteristic bands. However, the absorption of the chelate is so intense that the exciting radiation is absorbed within a few tenths of a millimeter after entering the solution. Therefore, only a small amount of the material in a laser cavity might be involved in laser action.

As a result, power and energy outputs are lower than those of conventional solid state lasers. Since this initial work, several other reports of rare earth chelate laser systems in which the ligand is involved in an energy transfer process have appeared. Bjorklund and co-workers obtained laser action from terbium tris(1,1,1-trifluoroacetylacetonate) at room temperature in acetonitrile and in dioxane.<sup>(8)</sup> These workers also reported the successful lasing of several other europium(III) chelate systems.<sup>(9)</sup> Schimitschek and co-workers studied the design of circulating laser systems using dimethylammonium salts of tetrakis europium-ortho-chlorobenzoyltrifluoroacetate dissolved in acetonitrile.<sup>(10)</sup> However, all these systems suffer the same deficiency as the first reported chelate systems - namely, that too much of the pumping light is absorbed by the outer surfaces of the liquid when contained in a laser cavity. In order to alleviate this difficulty, efforts in this laboratory have concentrated on the development of rare earth containing liquids in which the rare earth ion is excited directly.

During the course of this investigation, Heller reported a neodymium system based on the solvent selenium oxychloride-tin tetrachloride.<sup>(5)</sup> This system suffers from several deficiencies that are overcome by the phosphorus oxychloride system developed on this program. Considerable care must be taken in preparation of the selenium containing solutions due to the highly toxic nature of that element. Risk is also present in actual laser operation because of the possibility of breakage of the cell. In addition, best laser action in the  $\text{SeOCl}_2\text{-SnCl}_4$  system is obtained only with high concentrations of  $\text{SnCl}_4$ . However, a corresponding increase in viscosity also results from high  $\text{SnCl}_4$  concentrations and this leads to practical problems in the operation of a circulating liquid laser. Heller also reported the development of a neodymium laser using dimethylsulfoxide as the solvent and in which excitation is through the levels of neodymium(III). The laser active species is the o-phenanthroline adduct of neodymium pentafluoropropionate with at least one molecule of dimethylsulfoxide in the solvation shell. The large anion o-phenanthroline was used as the coordinating ligand to minimize the self-quenching effect of neodymium. Although this laser solution does offer some advantages over chelate systems, it has a limited shelf-life, presumably because of solvolysis of the adduct, and suffers from photodecomposition of dimethylsulfoxide by ultraviolet radiation (from the pumping source).

## II. DISCUSSION

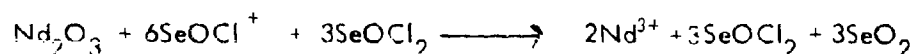
### A. THE NEODYMIUM III-PHOSPHORUS OXYCHLORIDE-TIN TETRACHLORIDE LASER

The approach used for this study of liquid laser parameters was to determine the influence of chemical and physical environmental factors upon the intensity, efficiency, and life-time of rare earth phosphorescence in liquid systems so that the most promising combinations of coordinating ligands, counter ions and solvents could be selected and evaluated in a laser cavity. In this regard, we have found that complex formation between different rare-earths and various  $O=PX_3$  type ligands results in a significant enhancement and selectivity of certain phosphorescent emissions. These ligands include triethylphosphate, tributylphosphate, hexamethylphosphoramide and phosphorus oxychloride. In each of these complexes the rare earth ion is probably surrounded by three  $Cl^-$  ions and three  $O=PX_3$  ligands so that the primary vibrational interaction involves the  $P=O$  stretching frequency at about  $1285\text{ cm}^{-1}$ . For  $Eu^{+3}$  (Figure 1) this vibrational quantum is not sufficiently energetic to interact effectively with the  $^5D_0$  emitting level since the smallest gap between  $^5D_0$  and even  $^7F_6$  is much greater (about  $12,000\text{ cm}^{-1}$ ) than the  $P-O$  vibrational quantum. A similar situation exists in  $Nd^{+3}$  where the lasing transition ( $^4F_3 \rightarrow ^4I_{11/2}$ ) is at  $9430\text{ cm}^{-1}$  and the lowest energy transition from the lasing emitting level is the  $^4F_{3/2} \rightarrow ^4I_{15/2}$  band at  $5500\text{ cm}^{-1}$ . In addition, the energy gaps between some of the initially excited levels and the lasing emitting level are about the same energy as the  $P-O$  vibration  $\sim 1080\text{ cm}^{-1}$ ,  $800\text{ cm}^{-1}$  and  $1200\text{ cm}^{-1}$  (see Figure 1). This would enable the emitting level to be populated by a cascade process as the upper levels could be depopulated by nonradiative interaction with the  $P-O$  vibrational frequency. For these reasons, neodymium was the rare earth ion of choice for lasing experiments.

Phosphorus oxychloride was the first solvent chosen for lasing studies of neodymium. The absorption spectrum for  $POCl_3$  was recorded in this laboratory from 200 to 3500 nm and found to be free of absorption bands between 500 and 2800 nm (Figure 2). The spectrum does contain a broad absorption between 2800 and 3500 nm characteristic of hydrogen bonded OH groups as an impurity and an increasingly broad absorption below 500 nm.

Phosphorus oxychloride would not interfere with direct neodymium pumping since 30% of the pumping is provided by levels in the near infrared, about 50% by the strong absorptions in the yellow and about 20% by the levels in the near ultraviolet. (12) Also, the solvent would not interfere with the  $\text{Nd}^{+3}$  lasing emission at 1056 nm. Ionic neodymium compounds should exhibit some solubility in  $\text{POCl}_3$  because of the moderate dielectric constant of this solvent, 13.9. The low viscosity of  $\text{POCl}_3$  (1.065 cP at 25° C) (13) suggested that a solution of neodymium in this solvent would be a promising system for a circulating liquid laser. The liquid range for  $\text{POCl}_3$  at atmospheric pressure is 1.25 to 105.8° C and would enable a laser to be operated under conventional conditions.

Initial work showed that the solubility of neodymium oxide in phosphorus oxychloride was negligible. This problem was similar to that encountered by Heller in the selenium oxychloride system. (5) He reported that neodymium oxide dissolved only to a limited extent in selenium oxychloride although that solvent has a high dielectric constant, 46.2. The solubility of neodymium oxide in selenium oxychloride increased when aprotic acids such as tin tetrachloride and antimony pentachloride were added. Heller postulated that  $\text{SnCl}_4$  reacts with  $\text{SeOCl}_2$  to form  $(\text{SeOCl}^+)_2 \text{SnCl}_6^{2-}$  and that the following reaction took place to dissolve the oxide.



Taking the same approach, we found that the addition of  $\text{SnCl}_4$  to mixtures of  $\text{POCl}_3$  and  $\text{Nd}_2\text{O}_3$  significantly increased the solubility of neodymium oxide. The absorption spectrum of tin tetrachloride was recorded between 300 and 3500 nm (Figure 3) and was found to be free of absorption bands between 500 and 2600 nm. Bands at 2750 and 2820 nm are characteristic of free OH groups of an impurity. An increasing broad absorption is also present in the spectrum of this material below 500 nm. Phosphorus oxychloride and tin tetrachloride react to give a 2:1 adduct (14) which is soluble in  $\text{POCl}_3$ . The absorption spectrum of such a solution was measured between 300 and 3500 nm (Figure 4) and was identical to the spectrum of  $\text{POCl}_3$ —the peaks for the OH

impurity in  $\text{SnCl}_4$  at 2750 and 2820 nm may be masked by the broader absorption due to  $\text{POCl}_3$  in this region.

In a typical preparation of a lasing solution, a mixture of neodymium oxide, phosphorus oxychloride and tin tetrachloride was refluxed for 24 hours. After this period, the mixture was cooled to room temperature and filtered under nitrogen pressure to remove undissolved neodymium oxide, undissolved 2:1 phosphorus oxychloride - tin tetrachloride adduct and any other reaction by-product. No attempt was made to dry the starting materials or to eliminate contact with atmospheric moisture. Transfers of tin tetrachloride and phosphorus oxychloride were carried out quickly in laboratory atmospheres. In this manner, a clear, pink solution of neodymium was obtained which was stable (no cloudiness developing) over the time periods - several months - during which they were stored. The concentration of  $\text{Nd}^{3+}$  was 0.15M and was determined using a new combined hydrolytic and spectrometric technique. (The details of this technique are given in the Appendix). The freezing point of the solution varied as a function of the  $\text{SnCl}_4$  content but exact relationships have not been determined. No crystallization occurs when the 0.15M lasing solution is cooled to  $0^\circ\text{C}$  for one hour.

The phosphorescent emission spectrum for this solution before lasing was recorded in the 830-1130 nm region with an Amico-Bowman Spectrophotofluorimeter at an excitation wavelength of 580 nm (Figure 5). The ratio of peak areas of the 1056 nm to 894 nm bands is 3:1. It would be interesting to obtain comparable data under identical instrumental conditions with other neodymium systems. The absorption spectrum in the 450-1000 nm region was recorded on a Beckman DK2A Spectrophotometer and the spectrum is shown in Figure 6. A sharp series of absorption peaks are present and the spectrum is quite similar to that reported by Heller for a solution of  $\text{Nd}^{3+}$  in  $\text{SnCl}_4\text{-SeOCl}_4$ .<sup>(15)</sup> An increasing broad absorption with decreasing wavelength due to the  $\text{POCl}_3\text{-SnCl}_4$  solvent mixture is apparent at the lower wavelengths.



Lasing in this  $\text{Nd}^{+3} - \text{POCl}_3 - \text{SnCl}_4$  solution was demonstrated in a quartz cell having a 1.2 cm bore and 12.5 cm path length with plane-parallel silica plates cemented on the ends. The cell was designed to occupy the same position in a commercial laser head that was normally occupied by a ruby rod. External quartz flat mirrors, one with a 90% reflective coating at  $1.06 \mu$  and the other with a totally reflecting dielectric coating, completed the laser cavity. Excitation was accomplished with unfiltered light from a helical air-cooled xenon flash lamp. The output from the cell was detected with a RCA 925 vacuum photodiode biased at 250 volts. The cathode was connected to ground through a 47 ohm load resistor. The signal was taken out across the 47 ohm resistor and fed into a Type O plug-in (max sens. = 1 mv) in a Type 545 Tektronix oscilloscope. A setting of 200 mv/cm on the vertical and 100  $\mu$  sec/cm on the time base usually was able to contain the output pulse. Stray visible and UV emission of the pump light was prevented from reaching the detector by taping a  $1.06 \mu$  interference filter across the detector aperture. The input threshold for the system was determined by firing the laser a number of times in succession and decreasing the input voltage each time. The repetition rate was standardized at 60 minutes to assure that the solution equilibrated to room temperature between flashes. The setting at which spiking disappeared was taken as the approximate input threshold. For the 1.2% by weight solution of  $\text{Nd}^{+3}$  in a  $\text{POCl}_3 - \text{SnCl}_4$  mixture (0.15N in  $\text{Nd}^{+3}$ ) the input threshold was found to be 1300 joules. This compared with a value of 1100 joules for a 4" x 3/8" diameter, 5% neodymium oxide-doped glass rod in the same cavity. The pulse duration was shorter for the liquid system than for the glass rod (0.5 msec versus 1.5 msec). Just above the threshold, incipient spiking begins as can be seen in Figure 7. Increasing the pumping power to 5000 joules with this solution produced the lasing output shown in Figure 8. Figures 9, 10, and 11 exhibit a regular "ringing" type of oscillatory  $1.06 \mu$  output whose intensity fluctuated with a period of 2  $\mu$ sec. Some preliminary measurements have been made on the degree of collimation of the output lasing beam. When the horizontal tubular quartz cell was half filled with the lasing solution, leaving a dry air bubble filling the top half of the cell length, the output beam retained the pattern of the liquid volume cross section for a long distance

beyond the exit end of the cell. Figure 12, which is a photograph of the orange spot on an Eastman IR Card intercepting the  $1.06\mu$  beam at 120 cm from the cell, shows that the semi-circular pattern of the beam cross section still matches the shape of the exit aperture of the lasing liquid. A solution was flashed 20 times in a preliminary study of the effect of flash input on physical properties. A slight increase in threshold was noted but this might be attributable to decay of other parts of the electronic and optical system. The only change in the appearance of the lasing solution was a slight darkening; there was no evidence of the formation of precipitate or cloudiness.

The absorption spectrum of the lasing solution in the 300-3500 nm range was recorded after lasing several times; the only change noted was a slight increase in background absorption. It has been reported that the presence of hydroxyl groups in the  $\text{Nd}^{3+}$  -  $\text{SeOCl}_2$  -  $\text{SnCl}_4$  system decreases the phosphorescence decay time from the lasing level.<sup>(16)</sup> Solutions prepared from anhydrous reagents had a longer phosphorescence decay time and superior laser action. The lasing experiments described above in the  $\text{POCl}_3$  system were conducted with solutions prepared with reagents that had not been purified. The use of anhydrous reagents for the preparation of lasing solutions in this system would probably improve the lasing characteristics.

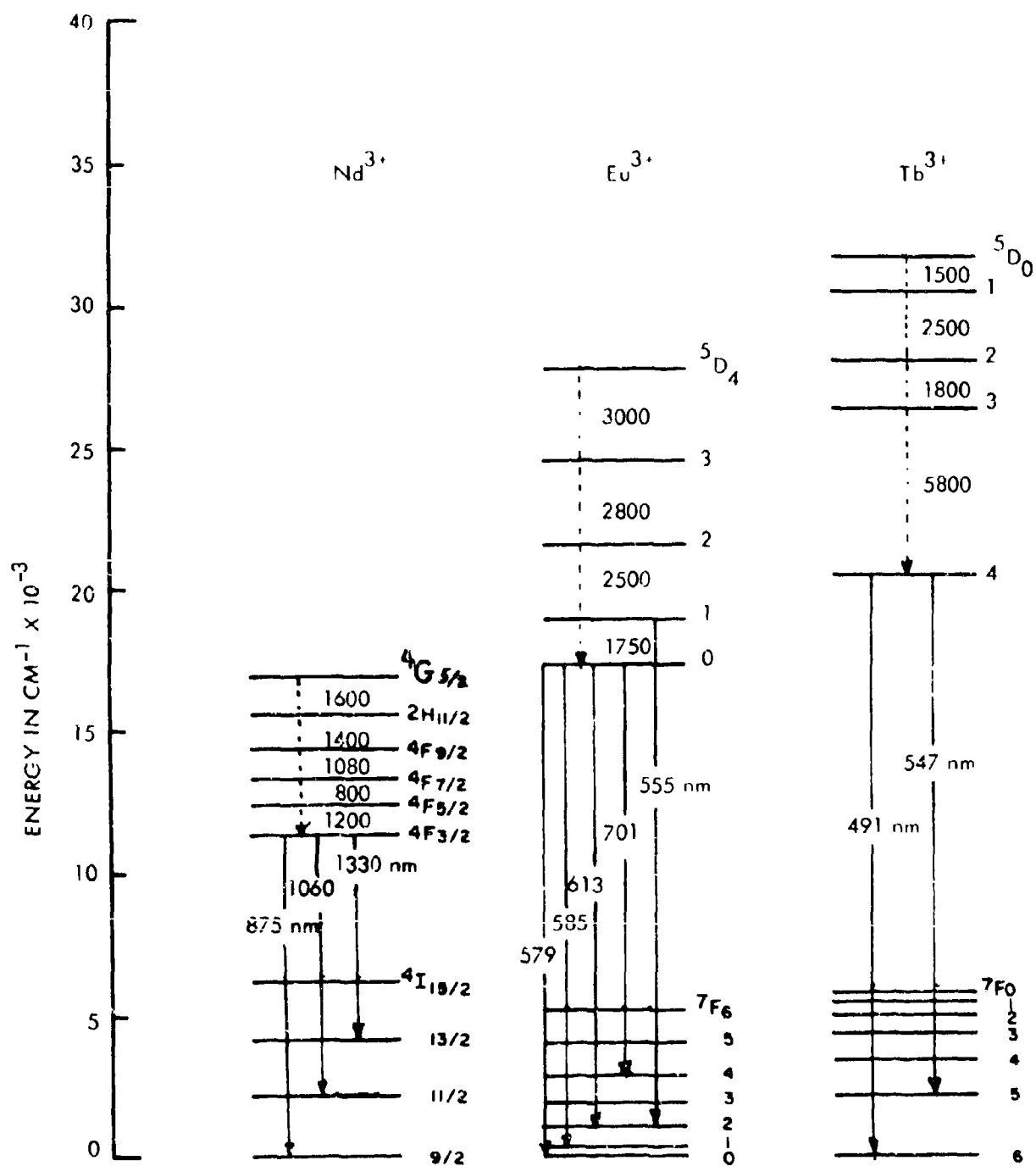
## B. EFFECT OF CHEMICAL ENVIRONMENT ON PHOSPHORESCENCE

### 1. Comparison of Phosphorescent Output of Rare Earths in $\text{H}_2\text{O}$ Versus $\text{D}_2\text{O}$

Kropp and Windsor have reported that substitution of  $\text{D}_2\text{O}$  for  $\text{H}_2\text{O}$  will enhance the phosphorescence of some rare earth solutions and this has been attributed to the decrease in the vibrational energy of O-D relative to O-H.<sup>(17)</sup> In this regard we examined the phosphorescence of  $\text{EuCl}_3$ ,  $\text{TbCl}_3$  and  $\text{SmCl}_3$  in  $\text{H}_2\text{O}$  and  $\text{D}_2\text{O}$  at room temperature in order to determine the enhancement effects of deuteration upon the principle emission bands of these ions. The energy level diagrams for these rare earths are found in Figure 1.

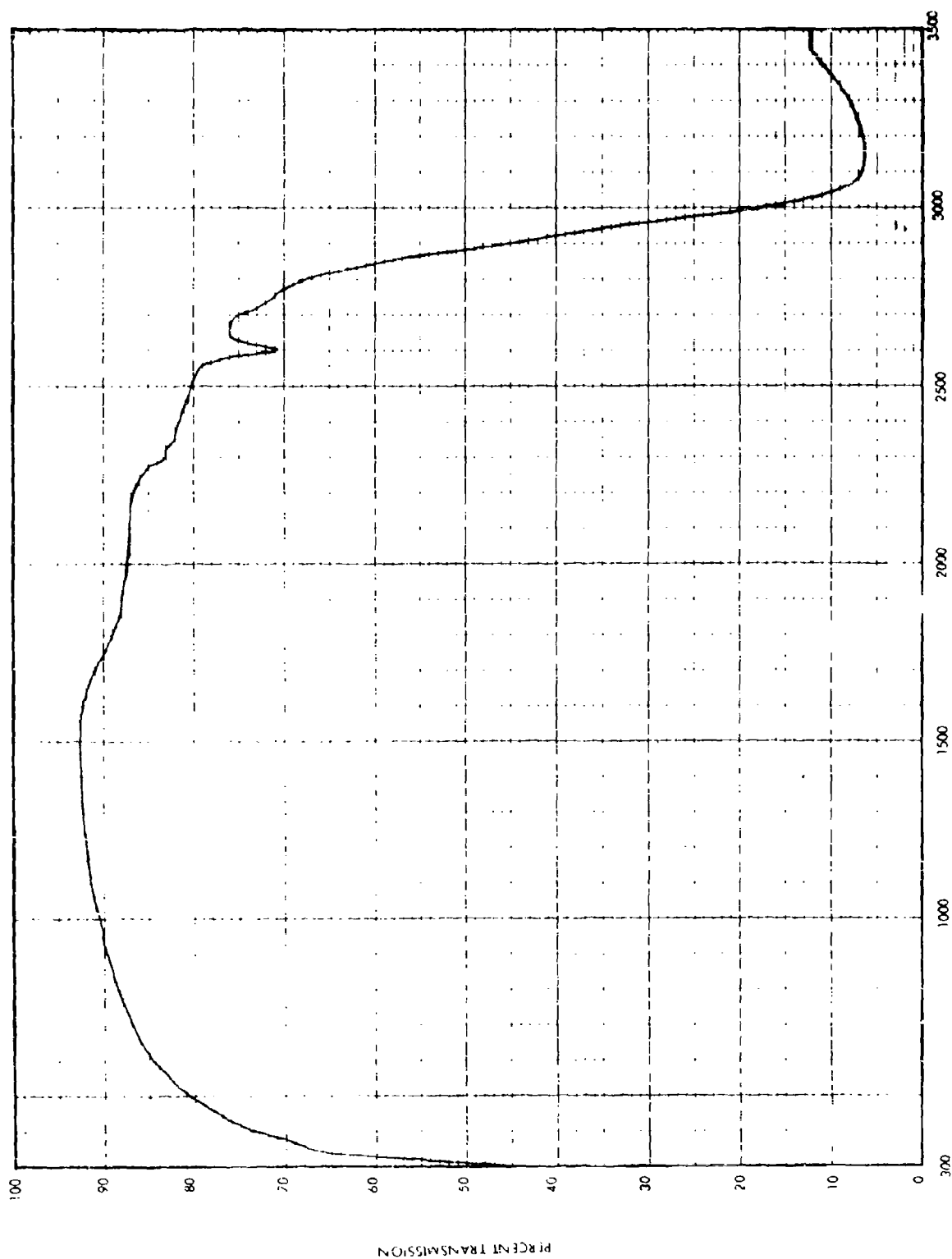
#### a. $\text{EuCl}_3$

The Eu (III) phosphorescence is especially interesting since there are two excited states



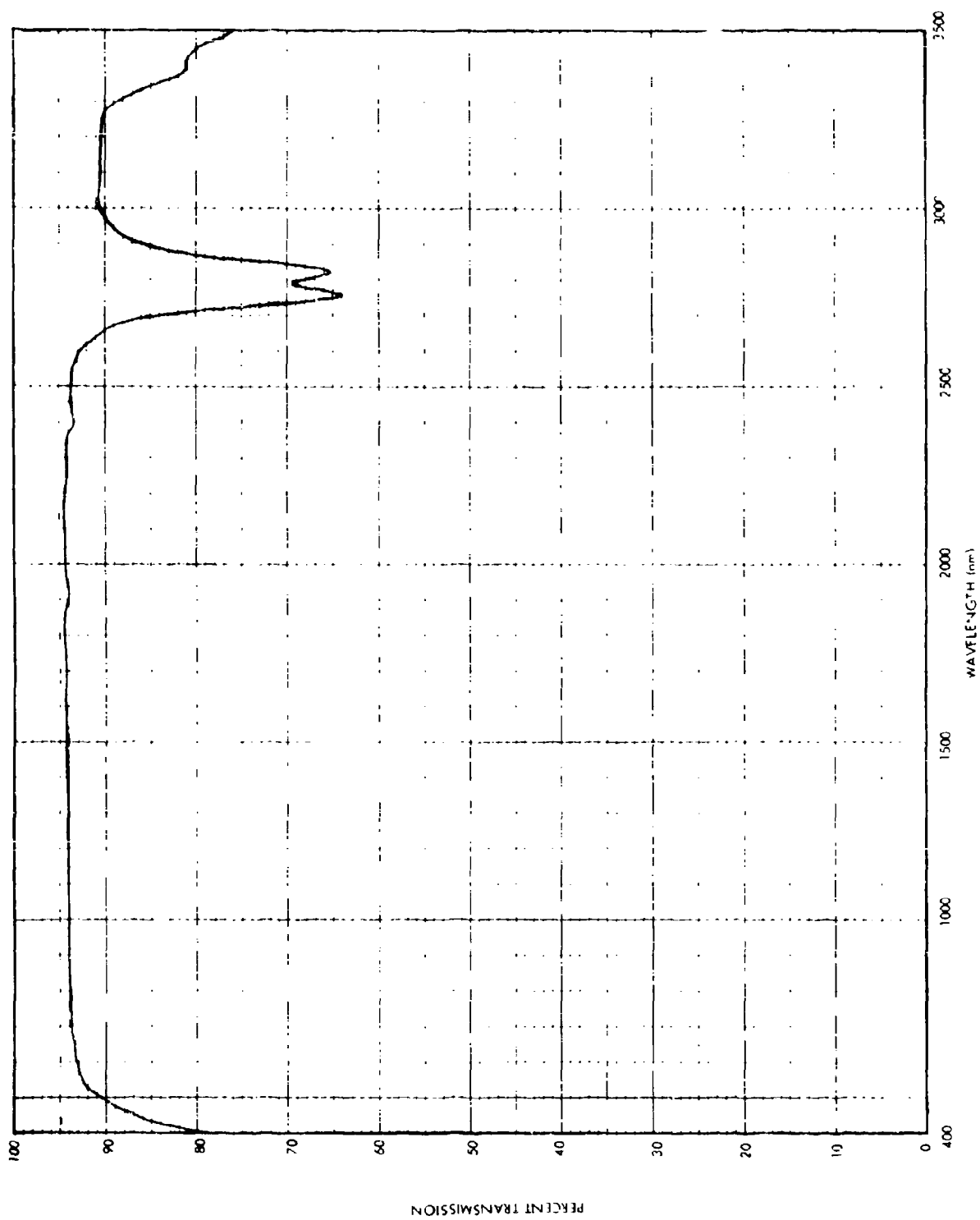
ENERGY LEVEL DIAGRAM FOR TRIVALENT Nd, Eu and Tb  
SHOWING MAJOR PHOSPHORESCENT TRANSITIONS

FIGURE 1



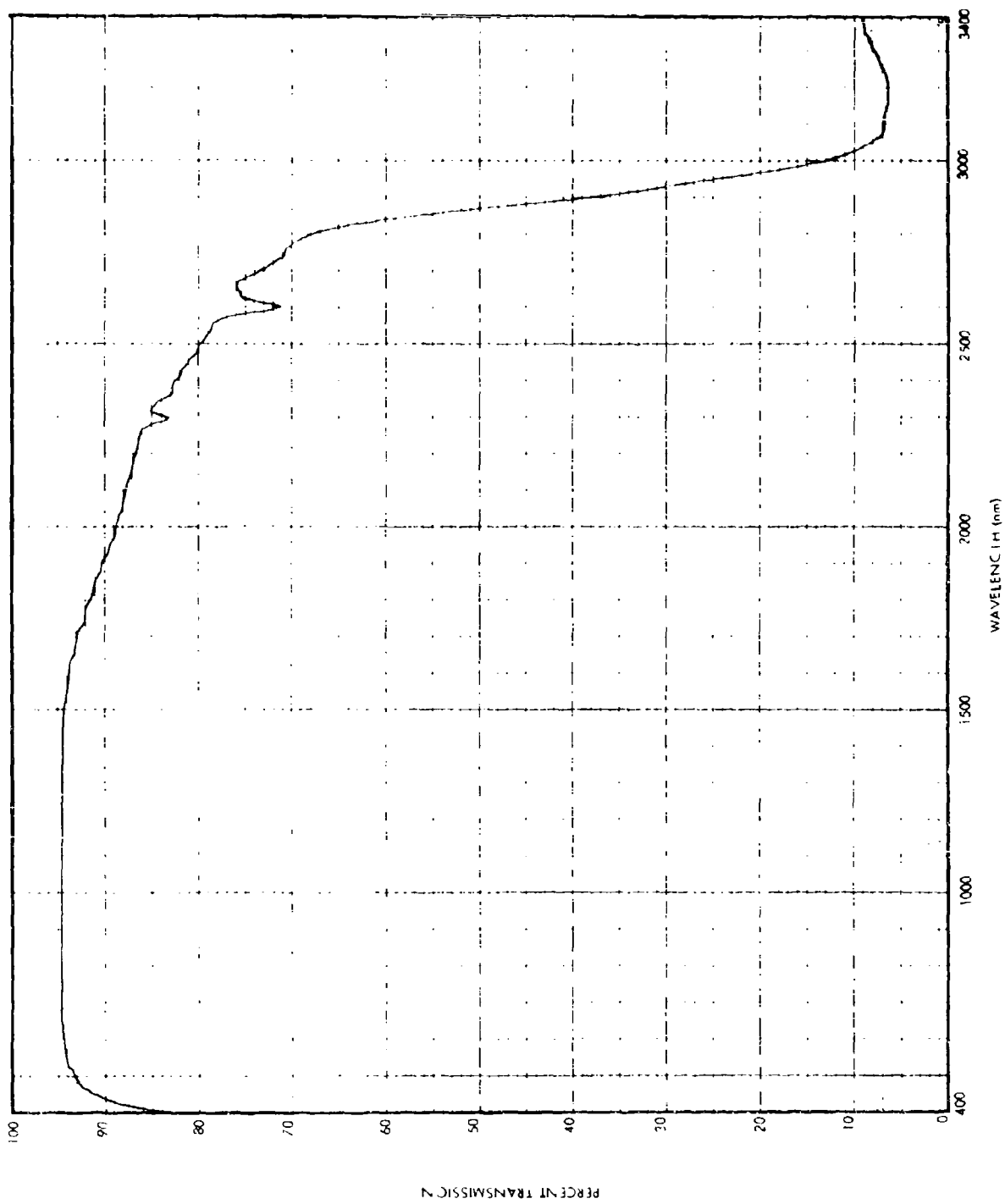
ABSORPTION SPECTRUM OF PHOSPHORIC ACID OXICHLORIDE

FIGURE 2



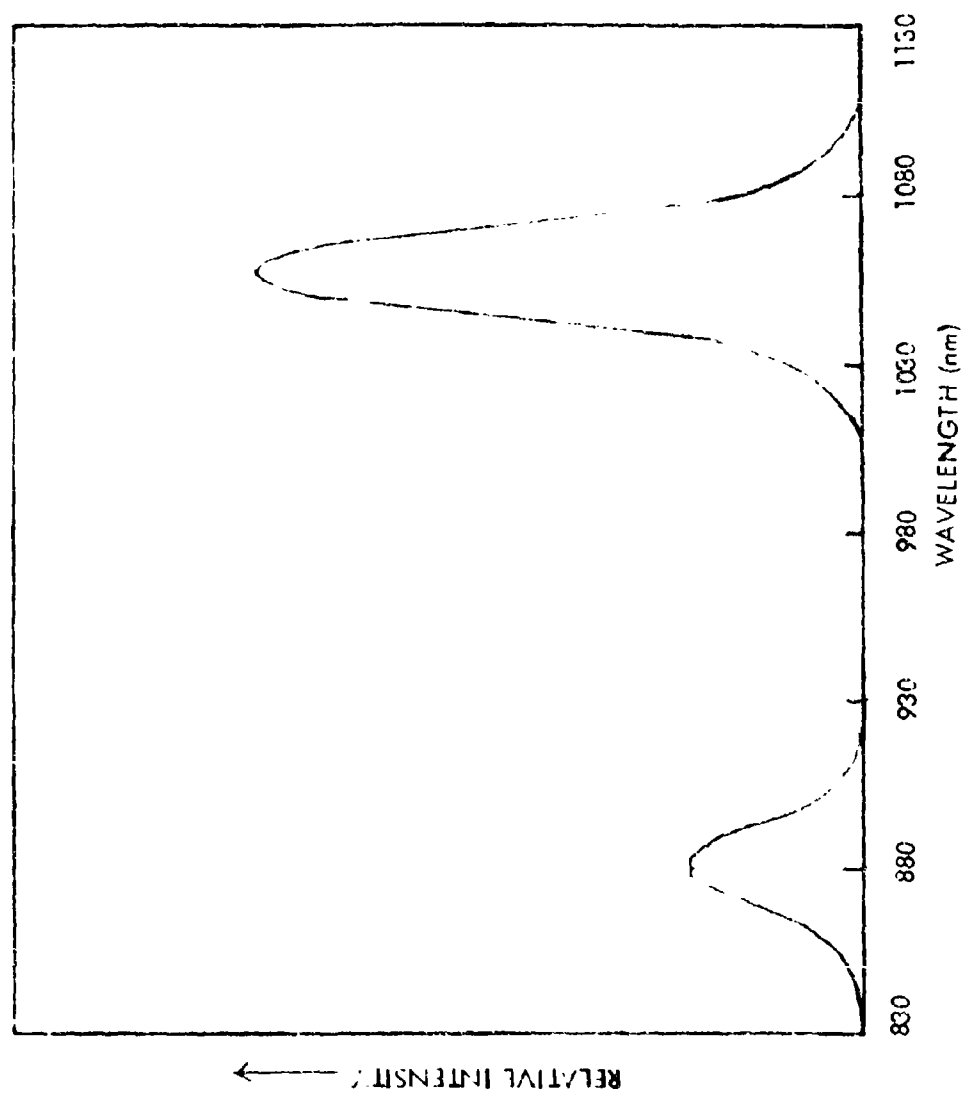
ABSORPTION SPECTRUM OF STANNIC CHLORIDE

FIGURE 3



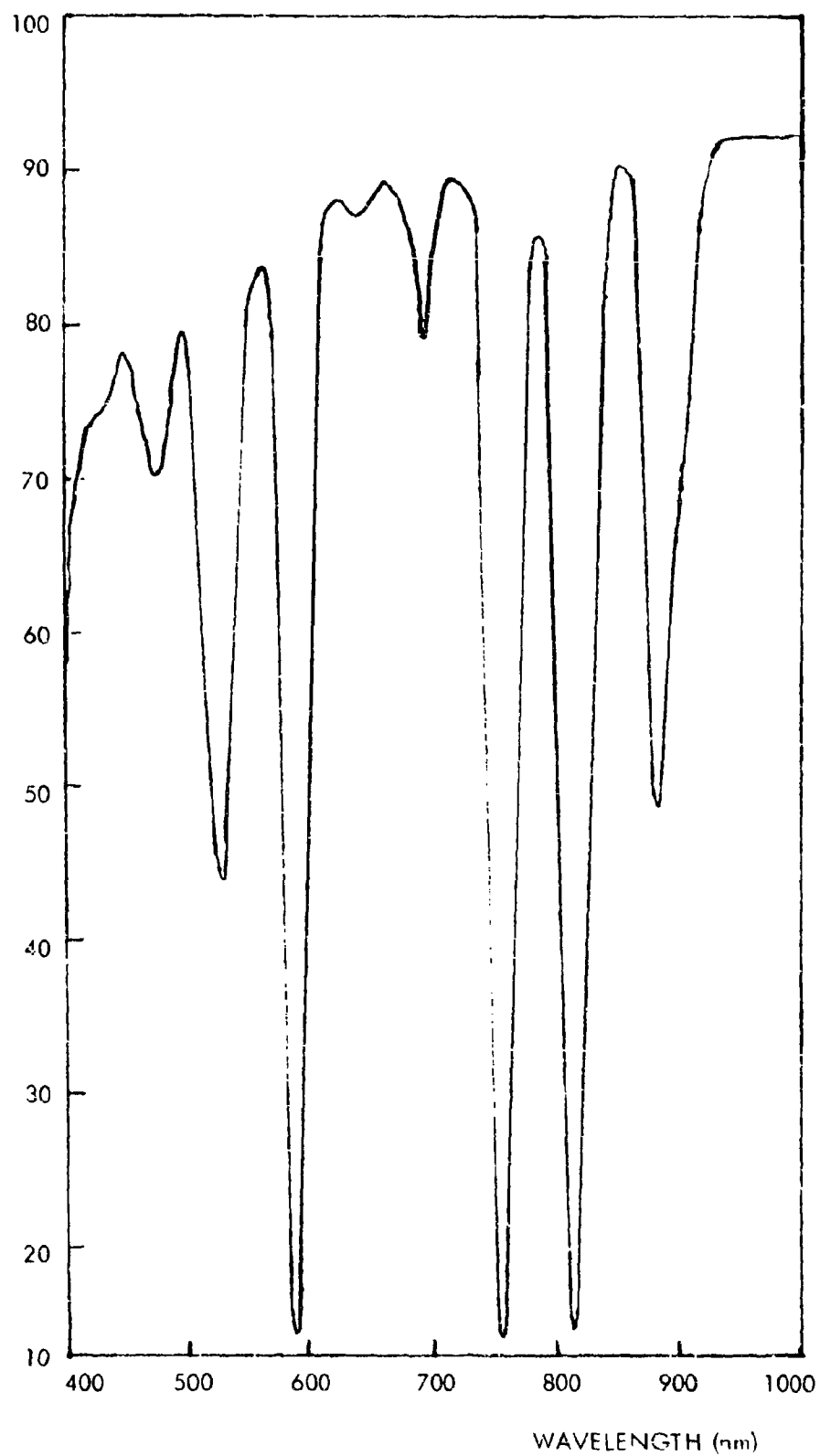
ABSORPTION SPECTRUM OF 5:1 VOLUME RATIO OF  $\text{POCl}_3$  TO  $\text{SnCl}_4$

FIGURE 4



PHOSPHORESCENCE SPECTRUM OF A SOLUTION OF  $\text{Nd}_2\text{O}_3$  (0.075M) IN THE SOLVENT SYSTEM  $\text{POCl}_3\text{-SnCl}_4$

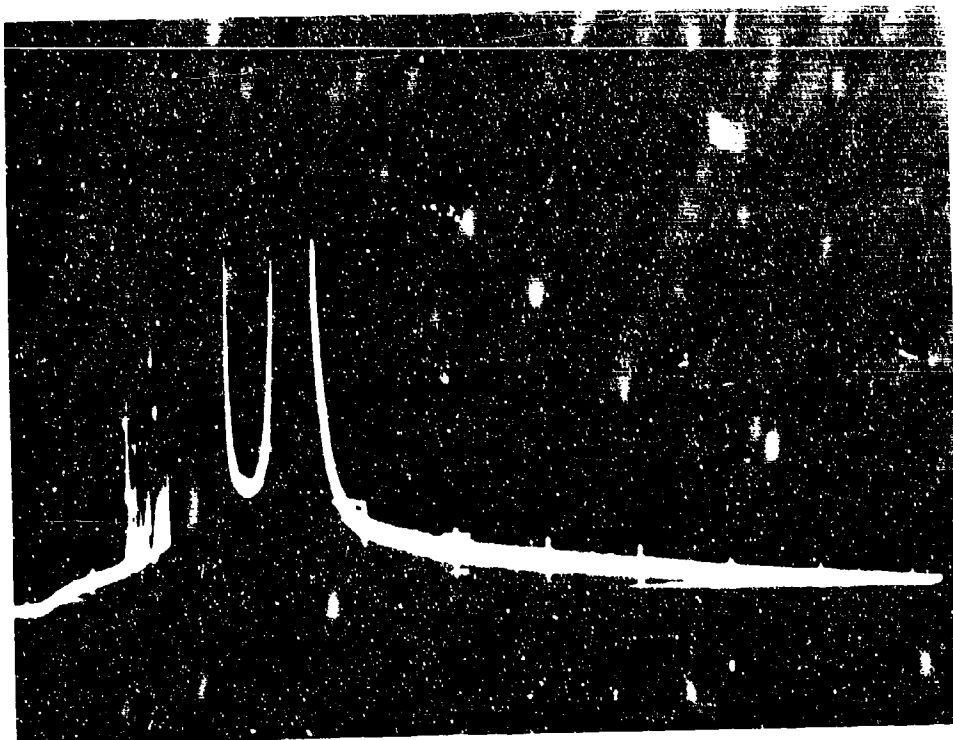
FIGURE 5



ABSORPTION SPECTRUM OF A SOLUTION OF  $\text{Nd}_2\text{O}_3$  (0.075Molar) IN THE SOLVENT SYSTEM  $\text{POCl}_3\text{-SnCl}_4$

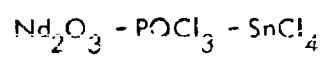
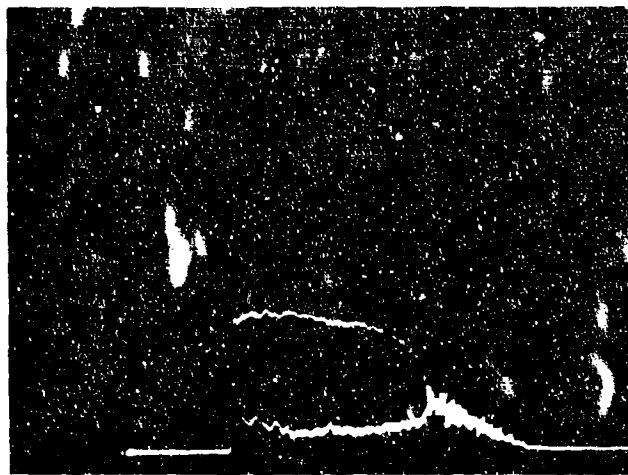
FIGURE 6





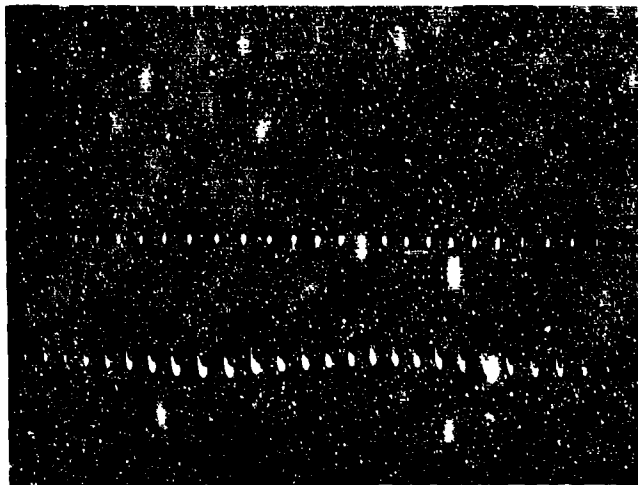
RANDOM SPIKING AT 1060 nm, 380 PERCENT  
ABOVE THRESHOLD  
INPUT: 5000J, 100 MICROSECONDS/cm

FIGURE 8



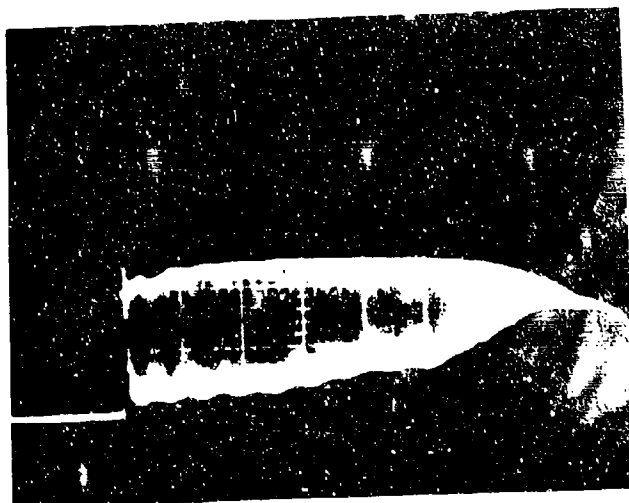
LIMIT CYCLE BEHAVIOR AT 1060 nm  
INPUT: 3000J, 100 MICROSECONDS/cm

FIGURE 9



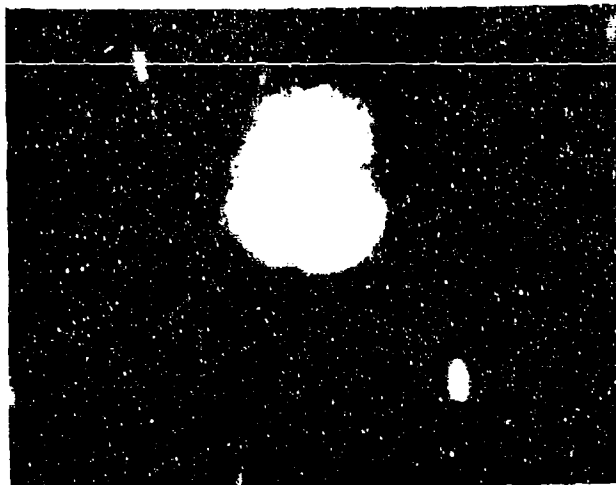
LIMIT CYCLE BEHAVIOR AT 1060 nm  
INPUT: 5000J, 50 MICROSECONDS/cm

FIGURE 10



$\text{Nd}_2\text{O}_3 - \text{POCl}_3 - \text{SnCl}_4$   
LIMIT CYCLE BEHAVIOR AT 1060 nm,  
EXPANDED TIME SCALE  
INPUT: 5000J, 5 MICROSECONDS/cm

FIGURE 11



DIRECT PHOTOGRAPH OF THE LASER BEAM  
SHOWING BEAM COLLIMATION

FIGURE 12

Polaroid photograph of the orange spot on an Eastman Kodak IR Card intercepting the lasing from 0.075M  $\text{Nd}_2\text{O}_3$  solution filling only the bottom half of the tubular horizontal quartz cell, with 5000 joules pump input. The Polaroid film was placed against the I. R. Card which was situated 120 cm from the output end of the cell.

from which detectable emissions can take place, namely  $^5D_0$  and  $^5D_1$ . Results of this work are showed in Table I. The phosphorescence of  $\text{EuCl}_3 \cdot 6\text{H}_2\text{O}$  in  $\text{H}_2\text{O}$  consists of three bands at 555 nm ( $^5D_1 \rightarrow ^7F_2$ ), 588 nm ( $^5D_0 \rightarrow ^7F_1$ ) and 619 nm ( $^5D_0 \rightarrow ^7F_2$ ). It can be seen from Table I that the dominant emission of  $\text{EuCl}_3 \cdot 6\text{H}_2\text{O}$  in  $\text{H}_2\text{O}$  arises from the magnetic dipole transition  $^5D_0 \rightarrow ^7F_1$ . The weaker  $^5D_0 \rightarrow ^7F_2$  band, the electric dipole transition, is indicative of a symmetric ligand environment with a center of symmetry and is consistent with a center of octahedral arrangement of the six water molecules. As seen in Table I, deuteration increases the phosphorescent intensity of all three emissions but the enhancement is much greater for the  $^5D_0 \rightarrow ^7F_1$  and  $^5D_0 \rightarrow ^7F_2$  bands than for the  $^5D_1 \rightarrow ^7F_2$  bands.

TABLE I  
Phosphorescence of  $\text{EuCl}_3$  in  $\text{H}_2\text{O}$  and in  $\text{D}_2\text{O}$

Emission Bands (nm)	Area Under Emission Curves (Arbitrary Unit) $\text{H}_2\text{O}$	$\text{D}_2\text{O}$	Enhancement Factor
555 ( $^5D_1 \rightarrow ^7F_2$ )	$0.24 \pm 0.02$	$0.39 \pm 0.04$	$1.6 \pm 0.3$
588 ( $^5D_0 \rightarrow ^7F_1$ )	$2.82 \pm 0.03$	$30.7 \pm 0.7$	$10.9 \pm 0.4$
619 ( $^5D_0 \rightarrow ^7F_2$ )	$0.46 \pm 0.04$	$5.73 \pm 0.15$	$12.5 \pm 1.5$

Freeman and co-workers reported that, for solid  $\text{EuCl}_3$  solvated with  $\text{H}_2\text{O}$  and  $\text{D}_2\text{O}$ , the phosphorescent lifetimes of both the  $^5D_1$  and  $^5D_0$  emissions were increased by a factor of 10 upon deuteration<sup>(18)</sup>. This is contrary to what is found in solution. In solution, the non-radiative relaxation of  $^5D_1 \rightarrow ^5D_0$  is apparently so fast that deuteration has not effectively reduced it as compared to the much slower  $^5D_0 \rightarrow ^7F_1$  relaxation. This suggested that enhancement of certain emission bands at the expense of others can be achieved by altering the chemical environment in liquid systems. Even though the

resolution of the spectra is too low to detect any of the crystal field splittings, the intensity ratio of the  $^5D_0 \rightarrow ^7F_1$  band relative to the  $^5D_0 \rightarrow ^7F_2$  band in  $H_2O$  and  $D_2O$  (6.1 versus 5.4) is relatively constant so that the symmetry of the ligand field about the Eu(III) ion has not been appreciably altered by deuteration. Further, the absorption spectra for  $EuCl_3 \cdot 6H_2O$  in  $H_2O$  and  $D_2O$  are identical and hence it may be concluded that only the non-radiative relaxation of the  $^5D_0$  state has been reduced. However, the lack of a similar enhancement for the  $^5D_1$  emission points out a basic difference between the non-radiative mechanisms of each excited state in solution.

b.  $SmCl_3$

The Sm(III) phosphorescence consists of two bands at 557 nm and 592 nm both of which originate from the same excited state. The enhancement factor in  $D_2O$  for each band is effectively the same (see Table 2) - 14.1 and 14.4. It has been reported that the  $D_2O$  enhancement effect seems to be inversely proportional to the energy difference between the emitting level and the next lower energy state (17). In the series Eu(III), Tb(III) and Gd(III) the enhancement factors are in the order Eu(III) > Tb(III) > Gd(III) while the energy differences increase in the opposite order. The energy difference for Gd(III) is in the ultraviolet range and consequently no  $D_2O$  enhancement was found. Sm(III) seems to follow this trend since its energy difference is less and the enhancement factor is greater than Eu(III). It is interesting to note when the energy difference between an emitting state and a next lower one becomes very small as in the case of  $^5D_1 \rightarrow ^5D_0$  the enhancement goes to zero. Therefore, there seems to be an optimum energy difference where the  $D_2O$  enhancement has its greater effect which is in the vicinity of Sm(III).

TABLE 2  
Phosphorescence of  $SmCl_3$  in  $6H_2O$  and in  $D_2O$

Emission Bands (nm)	Peak Intensity (Arbitrary Units)		Enhancement Factor
	<u><math>H_2O</math></u>	<u><math>D_2O</math></u>	
557	0.030	0.415	14.1
592	0.054	0.780	14.4

Excitation Wavelength = 400 nm

c.  $\text{TbCl}_3$ 

The results for  $\text{TbCl}_3 \cdot 6\text{H}_2\text{O}$  are more revealing. Table 3 lists the enhancement factors of four emission bands that were detected from the  $^5\text{D}_4$  excited state in  $\text{TbCl}_3 \cdot 6\text{H}_2\text{O}$  at two different excitation wavelengths. Also listed are the energy level transitions that correspond to the emission wavelengths based on the energy level diagram. It is to be noted that there seems to be a similar trend for the enhancement factor to decrease as the energy difference between the emitting and terminal states is increased. This is interesting since it indicates that there is a direct non-radiative relaxation mechanism between the excited  $^5\text{D}_4$  state and each of the four  $^7\text{F}$  terminal states. If there were only one relaxation process say  $^5\text{D}_4 \rightarrow ^7\text{F}_0$  (i.e. the highest energy state of the ground multiplet) the  $\text{D}_2\text{O}$  enhancement should not show any variation from one emission band to the next.

TABLE 3  
Phosphorescence of  $\text{TbCl}_3$  in  $\text{H}_2\text{O}$  and in  $\text{D}_2\text{O}$

Transition	Wavelength (nm)	Enhancement Factor	
$^5\text{D}_4 \rightarrow ^7\text{F}_6$	488	6.4	6.3
$^5\text{D}_4 \rightarrow ^7\text{F}_5$	543	6.6	6.5
$^5\text{D}_4 \rightarrow ^7\text{F}_4$	584	6.6	6.6
$^5\text{D}_4 \rightarrow ^7\text{F}_3$	618	7.0	7.1
Excitation Wavelength (nm)		350	369

In all of the above experiments anhydrous rare earth salts were not used and the  $\text{D}_2\text{O}$  was not of the highest isotopic purity. The O-H content for each of the solutions was estimated by infrared analysis and found to be about 15%. However, the significant points made above are not dependent upon any absolute value of the enhancement factor but rather involve relative effects which are encountered with each rare earth ion.



2. Comparison of the Phosphorescent Output of Europium in CH<sub>3</sub>OH, CH<sub>3</sub>OD and CD<sub>3</sub>OH

In the previous section, we found that in aqueous solutions of Eu<sup>+3</sup>, deuteration of the solvent enhances phosphorescence of the bands emanating from the <sup>5</sup>D<sub>0</sub> level (588 and 619 nm) but not the <sup>5</sup>D<sub>1</sub> level (555 nm). In this section, analogous effects in methanol solutions are reported. Solutions of EuCl<sub>3</sub> and EuCl<sub>3</sub> · 6H<sub>2</sub>O were prepared in the following solvents: CH<sub>3</sub>OH, CD<sub>3</sub>OH and CH<sub>3</sub>OD. The integrated intensities of the phosphorescence spectra of duplicate experiments are shown in Table 4.

The three solvents are isoelectronic, so that the ligand fields are identical. H (or D) is strongly bonded to carbon in a methyl group so that exchange of H (or D) on the methyl is negligible. The H (or D) of the hydroxyl group are labile and could exchange with any residual water.

The integrated phosphorescence intensities indicate that:

- a. As in water, deuteration (CH<sub>3</sub>OD) has little effect on the 555 nm band (<sup>5</sup>D<sub>1</sub> → <sup>7</sup>F<sub>2</sub>).
- b. Deuteration of the hydroxyl alone does produce enhancement of the <sup>5</sup>D<sub>0</sub> emission by factors of 5.7 for EuCl<sub>3</sub> and 4.6 for EuCl<sub>3</sub> · 6H<sub>2</sub>O.
- c. Deuteration of the methyl group (CD<sub>3</sub>OH) produces no appreciable enhancement of phosphorescence from any transition.

We conclude that the methyl hydrogens are too far removed from the Eu<sup>(+3)</sup> ion for their replacement by D to enhance the phosphorescence. The hydroxyl hydrogen is close enough to produce the enhancement, but since only one D atom is bonded to the oxygen rather than the two in D<sub>2</sub>O, the effect is correspondingly less. The ratio of the peak height of the 588 nm band to that of the 619 nm band, which is 8.5 in aqueous EuCl<sub>3</sub> solutions, is only about 1.5 in methanol solutions, regardless of isotopic composition. We attribute the slightly higher ratio in CD<sub>3</sub>OH to the higher water content of that solvent, which would also explain the slightly lower integrated fluorescence intensity. Additional work should be undertaken with the completely deuterated solvent, CD<sub>3</sub>OD, and with the corresponding ethanol derivatives to verify this result.

TABLE 4

Phosphorescence of Europium in Methanol and its Deuterium Substituted Derivatives

Solvent	Concentration ( $\text{Eu}^{+3}$ ) g cc $\times 10^3$	A *		h *
		555 nm	(579 + 588 + 613) nm	
		$\times 10^3$	$\times 10^3$	
$\text{CH}_3\text{OH}$	a. 10.6	4.72	111	1.56
	b. 8.3	3.61	146	1.63
$\text{CH}_3\text{OD}$	a. 10.6	4.72	631	1.48
	b. 8.7	4.60	670	1.45
$\text{CD}_3\text{OH}$	a. 11.8	4.25	74	2.38
	b. 10.6	5.65	104	2.66

a. Anhydrous  $\text{EuCl}_3$  in methanol

Concentration based on assumption that all of the salt dissolved.

b.  $\text{EuCl}_3 \cdot 6\text{H}_2\text{O}$  in methanol

A \* = 
$$\frac{\text{Area under emission curve (in}^2\text{)}}{\text{conc. (Eu}^{+3}\text{) g cc}}$$

h \* = ratio of peak height of 588 nm to peak height of 613 nm

1. Concentration of  $\text{Eu}^{+3}$  calculated on percentage of Eu in  $\text{EuCl}_3 \cdot 6\text{H}_2\text{O}$ 

2. The "h" ratio is uncorrected for variation in phototube sensitivity

3. Phosphorescence of Europium (III) Complexes with P-O Containing Ligandsa.  $[\text{EuCl}_3 \cdot 3 \text{O} \cdot \text{P(OR)}_3]$ 

The phosphorescence of europium in trialkylphosphate solutions was observed to be very intense. The phosphorescence spectrum of europium chloride in tributylphosphate (TBP) <sup>\*</sup> is shown in Figure 13 and displays the dominance of the  $^5\text{D}_0 \rightarrow ^7\text{F}_2$  transition. The resolution of this spectrum is not high, but the  $^5\text{D}_0 \rightarrow ^7\text{F}_0$  line is partially resolved from the  $^5\text{D}_0 \rightarrow ^7\text{F}_1$  band and a shoulder appears on the  $^5\text{D}_0 \rightarrow ^7\text{F}_2$  transition.

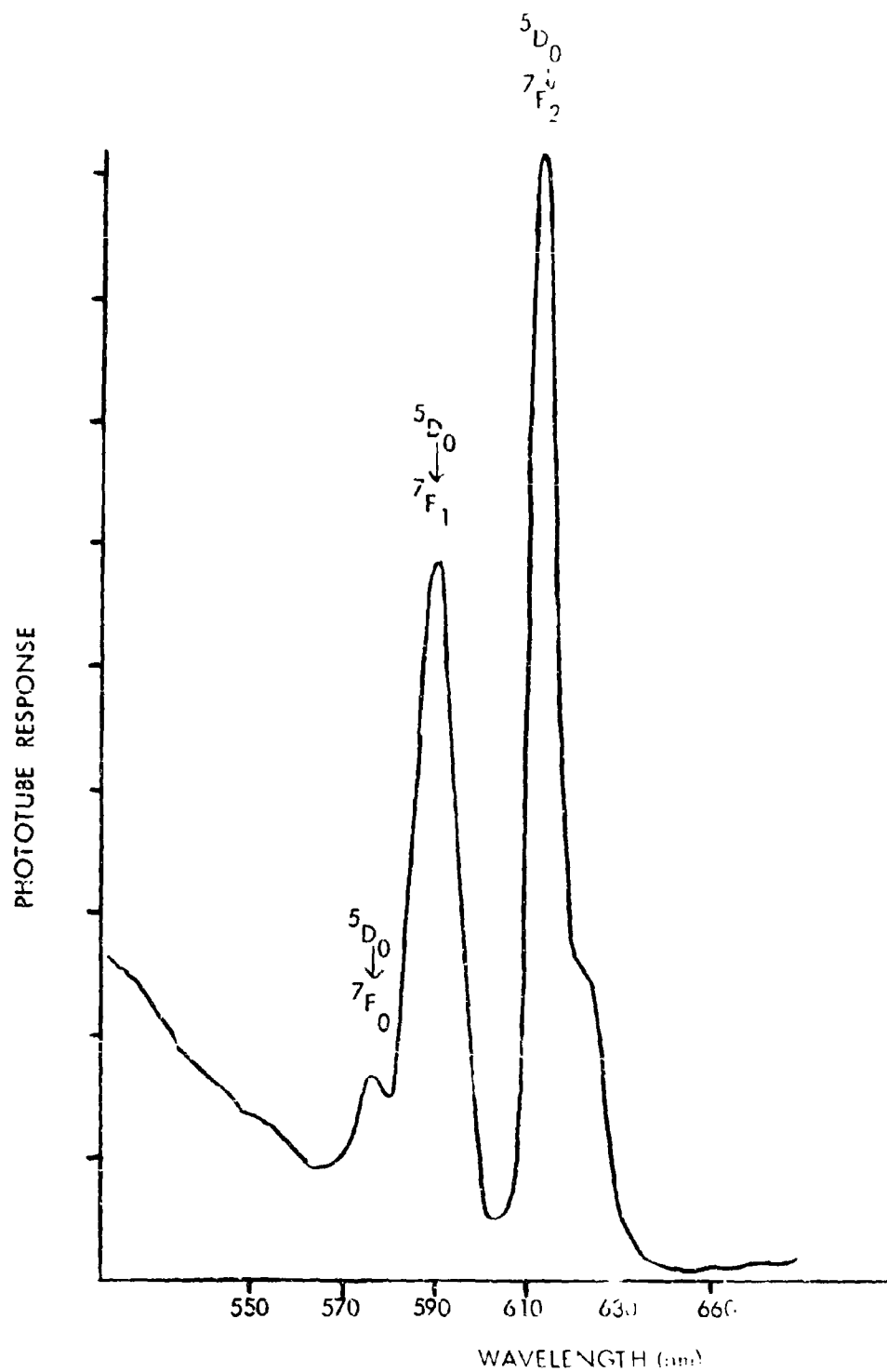
Figure 14 is the phosphorescence spectrum of  $\text{EuCl}_3$  in triethylphosphate (TEP) <sup>\*\*</sup> under the same resolution conditions as those used for tributylphosphate. Note that the relative intensity of the  $^5\text{D}_0 \rightarrow ^7\text{F}_2$  band in TEP does not show the shoulder noted in the corresponding TBP band. The  $\text{Eu}^{(+3)}$  environments in TBP and TEP therefore seem to be quite different in symmetry and possibly in the magnitude of the ligand field. This result is somewhat surprising since the structural differences between the two ligands are usually considered to be minor and far removed from the coordinating atom. One would expect little or no difference in the coordination characteristic and immediate ligand field about the  $\text{Eu}^{(+3)}$ . However steric factors arising from differences in the several alkyl groups may be important. Further work should be undertaken so that composition and structural assignments can be obtained and related to phosphorescence spectra.

In the  $\text{Eu}^{(+3)}\text{-TBP}$  complex, 79% of the detectable phosphorescence is in the  $^5\text{D}_0 \rightarrow ^7\text{F}_2$  transition and this represented our most successful effort to enhance the relative intensity of this band. However, we believe that other asymmetric complexes can be found in which the  $\text{Eu}^{(+3)}$  fluorescence is exclusively via this  $^5\text{D}_0 \rightarrow ^7\text{F}_2$  transition. Further, it is important to note that as we enhance the  $^5\text{D}_0 \rightarrow ^7\text{F}_2$  emission we also increase the transition probability of the  $^7\text{F}_0 \rightarrow ^5\text{D}_2$  absorption band. In considering any system as a potential laser, the absorption characteristics are just as important as the proper phosphorescence spectrum.

---

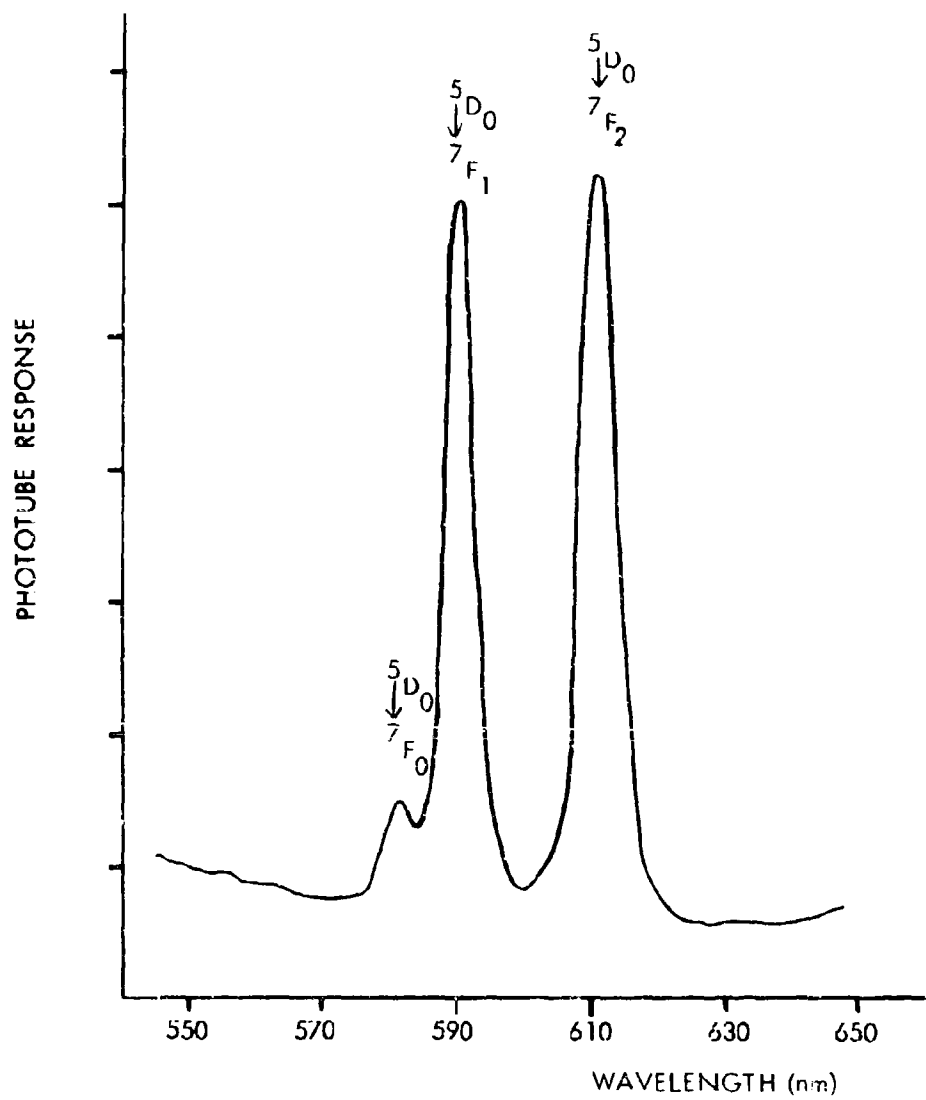
<sup>\*</sup> TBP: f. p.  $\sim -80^\circ \text{C}$ , b.p.  $289^\circ \text{C}$

<sup>\*\*</sup> TEP: f. p.  $-56^\circ \text{C}$ , b.p.  $215^\circ \text{C}$ .



PHOSPHORESCENCE OF EUROPIUM CHLORIDE IN TRIBUTYLPHOSPHATE

FIGURE 13



PHOSPHORESCENCE OF EUROPIUM CHLORIDE IN TRIETHYLPHOSPHATE

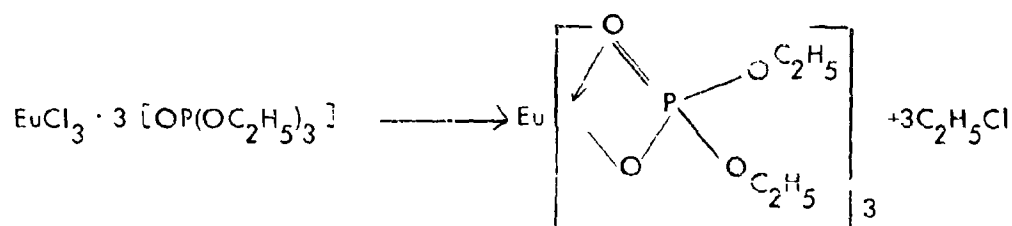
FIGURE 14

b.  $\text{Eu}[\text{O}_2\text{P}(\text{OR})_2]_3$ 

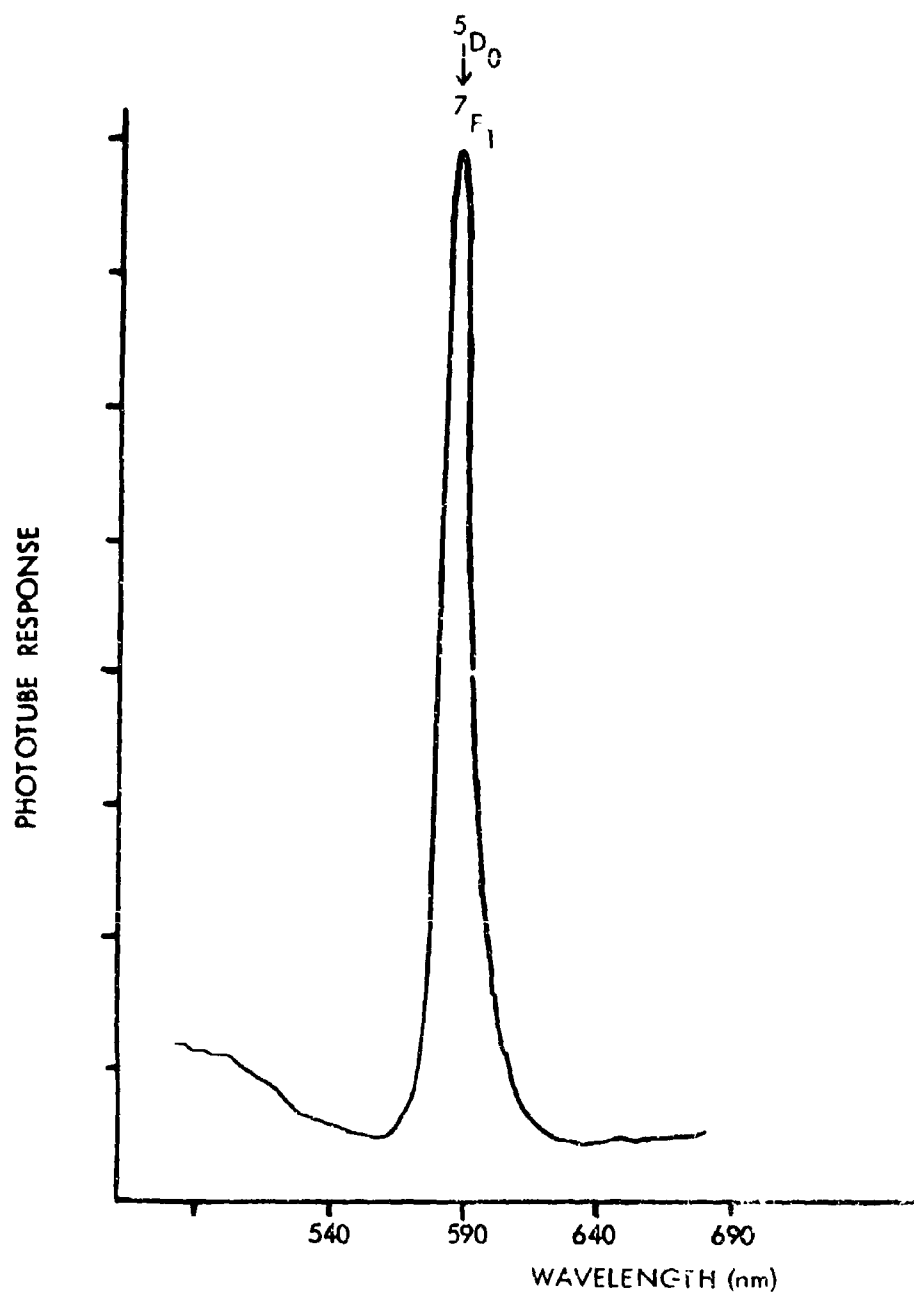
We discovered that a chlorine free complex is formed when  $\text{EuCl}_3 \cdot 3 \text{O}=\text{P}(\text{OR})_3$  complexes are decomposed by heating in excess solvent. These complexes have significantly different phosphorescent properties from the chlorine containing coordination compounds. The following procedure was followed in preparing the chlorine free complex derived from triethylphosphate. Some 30 ml of triethylphosphate was added to two grams of the hydrated rare earth chloride. The solution was heated with stirring at  $125^\circ \text{C}$  for two hours. After cooling, a 10:1 volume excess of anhydrous ethyl ether was added. The solution was cooled further to  $0^\circ \text{C}$  to complete the precipitation of the complex. After filtration, the precipitate was washed ten times with ether and then dried at  $110^\circ \text{C}$ . The elemental analysis of this complex is given below.

	%C		%H		%Cl		%P	
	Calc.	Obs.	Calc.	Obs.	Calc.	Obs.	Calc.	Obs.
$\text{Eu}[\text{O}_2\text{P}(\text{OC}_2\text{H}_5)_2]_3$	23.57	22.92	4.91	4.87	0.00	0.30	15.22	15.33
		23.28		5.04		0.10		15.19

The following reaction may have occurred with evolution of ethyl chloride.

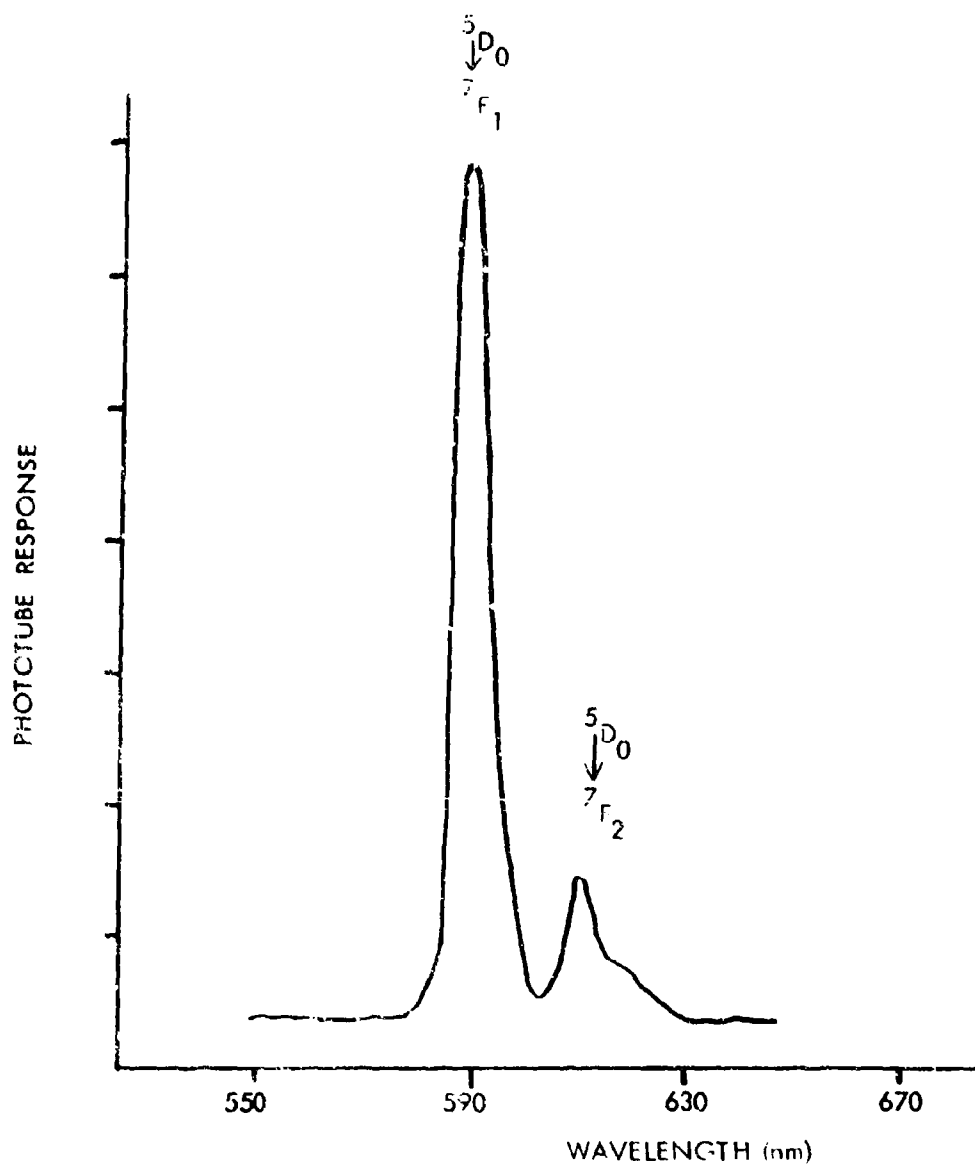


Additional studies would have to be undertaken to determine the structure of this complex and the reaction sequence. The phosphorescence spectrum of this complex is found in Figure 15 and consists only of a 592 nm band ( $^5\text{D}_0 \rightarrow ^7\text{F}_1$ ). No  $^5\text{D}_0 \rightarrow ^7\text{F}_2$  transition is apparent. The  $^5\text{D}_0 \rightarrow ^7\text{F}_0$  transition in the 575 nm region is too weak to detect. Essentially a decrease in both electric dipole transitions, i.e. the  $^5\text{D}_0 \rightarrow ^7\text{F}_0$  and the  $^5\text{D}_0 \rightarrow ^7\text{F}_2$  has occurred. This indicates the formation of a center of symmetry about the  $\text{Eu}(\text{III})$  in this complex.



PHOSPHORESCENCE OF  $\text{Eu}[\text{O}_2\text{C}(\text{OC}_2\text{H}_5)_2]_3$

FIGURE 15



PHOSPHORESCENCE OF  $\text{Eu}[\text{O}_2\text{P}(\text{OC}_4\text{H}_9)_2]_3$

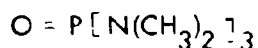
FIGURE 16



The  $\text{Eu}^{+3}$  - TBP system undergoes a similar conversion. The phosphorescence spectrum of the thermally ( $100^\circ \text{C}$ ) formed precipitate (Figure 16) is seen to be dominated by the  ${}^5\text{D}_0 \rightarrow {}^7\text{F}_1$  magnetic dipole transition. The  ${}^5\text{D}_0 \rightarrow {}^7\text{F}_2$  electric dipole transition accounts for about 37% of the total fluorescence as compared to 79% for the unconverted  $\text{EuCl}_3$ -TBP complex (Figure 13). This drastic change in the relative intensity of  ${}^5\text{D}_0 \rightarrow {}^7\text{F}_2$  transition indicates again that a symmetry conversion of the TBP ligand field about the  $\text{Eu}^{(+3)}$  has taken place.

c.  $\text{EuCl}_3 \cdot 3$  Hexamethylphosphoramide

Hexamethylphosphoramide (HMPA) \* has the following structure



A europium complex was prepared in the following manner. Two grams of the hydrated rare earth chloride was added to 30 ml of the complexing agent. The solution was heated with stirring at about  $100$ – $125^\circ \text{C}$  for two hours. After cooling, a 10:1 volume excess of anhydrous ethyl ether was added. The solution was cooled further to  $0^\circ \text{C}$  to complete the precipitation of the complex. After filtration, the precipitate was washed ten times with ether and then dried. The elemental analysis indicates three ligand molecules bonded to the original molecule.

	<u>%C</u>	<u>%H</u>	<u>%N</u>	<u>%Cl</u>	<u>%P</u>
Calcd. for $\text{EuCl}_3 \cdot 3\text{HMPA}$	27.16	6.79	15.84	13.38	11.69
Found	26.92	6.62	15.65	13.37	11.49

In order to gain some information about the influence of the solvent on the nature of the emission spectra and on the magnitude of the phosphorescent intensity, an investigation of solutions of  $\text{EuCl}_3 \cdot 3\text{HMPA}$  in various solvents, particularly some alcohols, was undertaken. The results are summarized in Table 5. The emission spectra of these systems consisted generally of the 588 and 619 nm bands. No attempt was made to resolve these bands and little can be said about the symmetry surrounding the emitting species. The first solvent used was HMPA itself and its phosphorescence spectrum taken under high resolution revealed to be identical to the solid material except for a slight broadening of the emission bands.

\* Hexamethylphosphoramide is a room temperature liquid with a boiling point of  $80^\circ \text{C}$  (at 3 mm).

This indicates that the crystal field is essentially the same and that no further coordination by the HMPA occurs.

A comparison of the data in different solvents indicates the following:

1. The total fluorescence intensity from  $\text{EuCl}_3 \cdot 3\text{HMPA}$  is greater by a factor of about 3 in HMPA and  $\text{CH}_3\text{OH}$  than in any of the other solvents used.
2. Varying the chain length of the solvent alcohol doesn't appear to have any important effect on the phosphorescent intensity; if anything, it reduces it (cf.  $\text{CH}_3\text{OH}$  and  $\text{C}_2\text{H}_5\text{OH}$ ).
3. It is evident from the variation in the 588/619 ratio that either a different symmetry exists about the  $\text{Eu}^{+3}$  or that different absorbing species are present in the HMPA and  $\text{H}_2\text{O}$  systems. Similarly either a difference in the symmetry or different absorbing species exist in the water and alcohol systems.

d.  $\text{EuCl}_3 \cdot \text{XPOCl}_3$

This compound was prepared by the method outlined in a previous section for the triethylphosphate complex using 30 ml of phosphorus oxychloride and two grams of the hydrated rare earth chloride. In the preparation of the phosphorus oxychloride complex of  $\text{Eu(III)}$  some difficulty was experienced in the apparent hydrolysis of the  $\text{EuCl}_3 \cdot \text{XPOCl}_3$  upon standing in air. The infrared spectrum of the  $\text{EuCl}_3 \cdot (\text{POCl}_3)_x$  compound contained a P-Cl band at  $580 \text{ cm}^{-1}$ , presumably a P-O-Eu band at  $1225 \text{ cm}^{-1}$  but no indication of any P-O-H absorption. The P-Cl and P=O bands in phosphorus oxychloride are at  $570 \text{ cm}^{-1}$  and  $1285 \text{ cm}^{-1}$  respectively, which indicates a shift of about  $60 \text{ cm}^{-1}$  toward lower energy in the phosphorus to oxygen band upon complex formation. Similar shifts were noted in the HMPA and TEP complexes. An elemental analysis of the  $\text{EuCl}_3 \cdot \text{XPOCl}_3$  complex was not attempted because of its hydrolytic instability. The phosphorescence spectrum of this material consisted almost entirely of the red multiplet  $^5\text{D}_0 \rightarrow ^7\text{F}_2$ . The symmetry of the crystal field must therefore be very low, since this transition is split into its maximum number of components, namely five. The band is about  $120 \text{ \AA}$  wide with components at  $6107 \text{ \AA}$ ,  $6127 \text{ \AA}$ ,  $6148 \text{ \AA}$ ,  $6204 \text{ \AA}$ , and  $6227 \text{ \AA}$ . The absence of the  $^5\text{D}_0 \rightarrow ^7\text{F}_1$  transition is quite promising since it again implies a highly efficient selection process governing the transition to the ground state.

TABLE 5  
Effect of Solvent on the Phosphorescence of  $\text{EuCl}_3 \cdot 3\text{HMPA}$

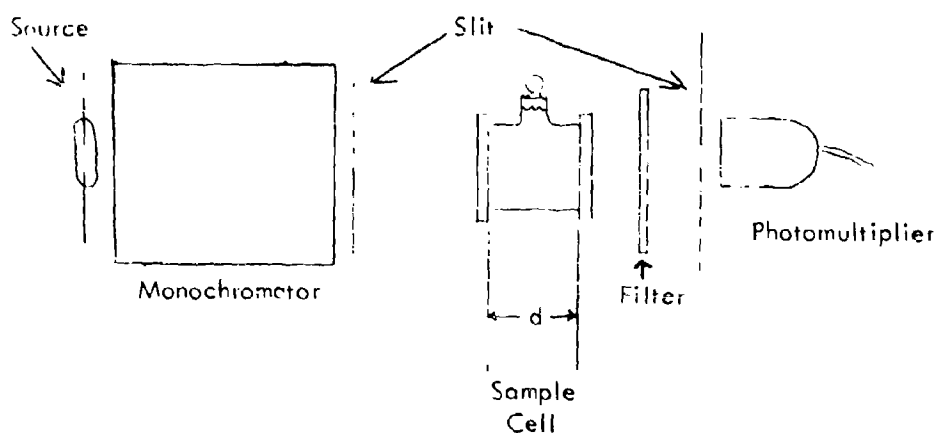
<u>Solute</u>	<u>Solvent</u>	<u>mg <math>\text{Eu}^{+3}/\text{cc}</math></u>	<u><math>\lambda_{\text{ex}}</math> (nm)</u>	<u>Relative Peak Areas 588/614</u>	<u>A *</u>
$\text{EuCl}_3 \cdot 6\text{H}_2\text{O}$	$\text{H}_2\text{O}$	45.2	390	8.25	
$\text{EuCl}_3 \cdot 3\text{HMPA}$	$\text{H}_2\text{O}$	2.1	391	8.23	1.0
$\text{EuCl}_3 \cdot 3\text{HMPA}$	$\text{H}_2\text{O}$	29.1	391	6.25	0.44
$\text{EuCl}_3 \cdot 3\text{HMPA}$	$\text{H}_2\text{O} + \text{HMPA} (2/1)$	4.6	391	3.78	0.96
$\text{EuCl}_3 \cdot 3\text{HMPA}$	HMPA	5.64	391	1.02	3.6
$\text{EuCl}_3 \cdot 3\text{HMPA}$	HMPA	5.64	461	1.03	8.2
$\text{EuCl}_3 \cdot 3\text{HMPA}$	HMPA	5.64	530	1.02	2.7
$\text{EuCl}_3 \cdot 3\text{HMPA}$	$\text{CH}_3\text{OH}$	2.5	391	1.12	3.8
$\text{EuCl}_3 \cdot 6\text{H}_2\text{O}$	$\text{CH}_3\text{OH}$	31.8	395	1.76	0.95
$\text{EuCl}_3 \cdot 3\text{HMPA}$	$\text{C}_2\text{H}_5\text{OH}$	2.52	391	1.0	0.88
$\text{EuCl}_3 \cdot 3\text{HMPA}$	$i\text{-C}_3\text{H}_7\text{OH}$	2.50	391	0.8	0.96
$\text{EuCl}_3 \cdot 3\text{HMPA}$	$i\text{-C}_3\text{H}_7\text{OH}$	2.50	461	0.78	2.0
$\text{EuCl}_3 \cdot 3\text{HMPA}$	$n\text{-C}_5\text{H}_{11}\text{OH}$	2.50	391	1.34	0.86
$\text{EuCl}_3 \cdot 3\text{HMPA}$	$(\text{CH}_2\text{OH})_2$	2.48	391	2.36	1.24

A \* = Integrated emission area of 588 + 614 ( $\text{in}^2$ )/C \* (total fluorescence)

T = 24° C

e. Quantum Efficiency Measurements of  $\text{Eu}^{3+}$  - TEP Solutions

The experimental set-up for the quantum efficiency measurement is shown below. The output of a xenon lamp is passed through a monochromator so that a particular exciting wavelength can be selected, and focused onto the sample. A photomultiplier is placed behind a slit which is directly in line with the exciting beam emerging from the sample. The number of quanta absorbed ( $\Delta n_2$ ) can be easily determined by comparing the transmission of the sample to that of the solvent. It is necessary that the photomultiplier slit be sufficiently wide to enable all of the exciting beam to strike the photomultiplier. The fluorescence signal is negligible compared to the transmitted signal, and so no filter is needed when measuring  $\Delta n_2$ . A calibrated neutral density filter was placed at the exit slit of the monochromator to reduce the intensity of the transmitted beam to the detection limits of the photomultiplier. The absorption coefficients measured by this method compare very well with those obtained with a Beckman DK2A absorption spectrometer.



To determine  $\Delta n_f$ , the number of fluorescent quanta, is not quite so simple, since the fluorescence is isotropically emitted over the solid angle of  $4\pi$ . However, by measuring the fluorescence passing through the slit of area  $A$  and then integrating along the length of the excited sample the following expression for  $\Delta n_f$ , can be developed;

$$F = \frac{\phi P_o k^2 A e^{-kr}}{4\pi} \left[ \frac{e^{k(r-d)}}{k(r-d)} - \frac{e^{kr}}{kr} + Ei(kr) - Ei(kr+kd) \right] \quad (1)$$

where  $F$  the detected fluorescence signal  
 $\phi$  overall quantum efficiency  
 $P_o$  incident exciting radiation  
 $k$  absorption coefficient in  $\text{cm}^{-1}$   
 $r$   $d - x$   
 $Ei(x)$  tabulated values of  $\int_{-\infty}^x \frac{e^x}{x} dx$

When measuring the fluorescence radiation, a Corning CS3-67 sharp cut-off filter must be used so that none of the exciting radiation strikes the photomultiplier. Further, no neutral density filter was used when measuring  $F$ .

Expression (1) enables one to calculate the absolute quantum efficiency in terms of the geometry of the experimental arrangement and the absorption characteristics of the sample which are all determinable. In our experiment a calibrated 1P21 photomultiplier was used to detect  $F$  and  $P_o$ . Since the two radiations are not at the same wavelength, the spectral characteristics of the detector must be considered. In the derivation of Equation (1) it has been assumed that the fluorescence is isotropic and losses due to scattering and absorption are negligible. Using Equation (1) we have calculated the quantum efficiency of an alcoholic Rhodamine B solution and of  $\text{Eu}(\text{NO}_3)_3$  in TEP. The results for the Rhodamine B solution, which is known to have a quantum efficiency of about 0.90 yield, yield a  $\phi$  which is too low by a factor of about 10. We have not determined why these results are low, but we can still obtain relative quantum efficiencies using Rhodamine B as a standard.

Equation (1) yields a simple expression for the  $\text{Eu}^{+3}$  - TEP fluorescence relative to that of Rhodamine B. If the concentrations of  $\text{Eu}(\text{NO}_3)_3$  in TEP and Rhodamine are adjusted so that the absorption coefficients  $k$  are identical at the same excitation wavelength  $\lambda_0$ , then we have the relationship that:

$$\frac{F'_{\text{Eu}}}{F'_{\text{Rh}}} = \frac{\phi_{\text{Eu}}}{\phi_{\text{Rh}}} \quad (2)$$

where  $F'_{\text{Eu}}$  and  $F'_{\text{Rh}}$  are the corrected fluorescences, detected with the same slit, for  $\text{Eu}^{+3}$  and Rhodamine solutions, respectively. The adjustment of the concentrations was carried out on the same apparatus so that no discrepancies due to different band widths would occur. The results of the relative experiment indicate that the  $\text{Eu}^{+3}$  - TEP solution has overall quantum efficiency of about 0.50 (50%) when the excitation wavelength is 395 nm. The quantum efficiency of the 465 nm band has not been determined but we believe that it will be at least as great since the level immediately excited is closer to the  $^5\text{D}_0$  level. We are losing one-half of the metastable states which never emit fluorescence and are primarily dissipated through useless non-radiative processes. This value of 0.50 is taken to be typical for  $\text{X}_3\text{P}=\text{O}$  complexes of  $\text{Eu}^{+3}$ , since we feel that the quantum efficiency is determined by interactions with the immediate environment about the rare-earth-ion. Using this result we can now proceed to the threshold power level calculation.

#### 4. Complexes of Rare Earths with Dimethylacetamide and its Homologs

##### a. Preparation and Characterization of Complexes of $\text{Eu}^{+3}$ , $\text{Tb}^{+3}$ , and $\text{Nd}^{+3}$

In order to understand exactly how the chemical environment of the rare earth ion affects the phosphorescence, it is critical to establish just what that environment is. The procedure described below was followed to prepare complexes of rare earths with dimethylacetamide. A distillation train was set up which was continually purged with dry nitrogen, and solvents were distilled from various drying agents. An inert atmosphere box was procured for the actual sample preparation. Hydrated rare earth

salts were dissolved in pure solvent and the excess solvent was then driven off under vacuum, leaving crystals of the rare-earth-ligand-solvent complex. This process was repeated leaving crystals analytically pure and virtually water-free. The samples were then sent to Galbraith Laboratories for compositional analysis.

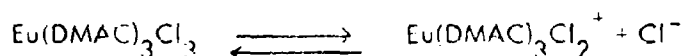
The first samples of the corresponding Nd, Tb and Eu complex were prepared and analyzed, and the results are given in Table 6. The theoretically calculated values are based on three dimethylacetamide ligands and three chloride ions. The analyses indicate that the molecular formulas for these complexes are thus:  $\text{Eu}(\text{DMAC})_3\text{Cl}_3$ ,  $\text{Tb}(\text{DMAC})_3\text{Cl}_3$ , and  $\text{Nd}(\text{DMAC})_3\text{Cl}_3$ .

TABLE 6  
Elemental Analyses of DMAC Complexes

		<u>% C</u>	<u>% H</u>	<u>% N</u>	<u>% Cl</u>
$\text{Eu}(\text{DMAC})_3\text{Cl}_3$	Calc.:	27.8	5.21	8.11	20.5
	Found:	28.8	5.77	8.56	19.2
$\text{Tb}(\text{DMAC})_3\text{Cl}_3$	Calc.:	27.4	5.13	7.99	20.3
	Found:	26.0	5.19	7.70	19.9
$\text{Nd}(\text{DMAC})_3\text{Cl}_3$	Calc.:	28.2	5.27	8.21	20.8
	Found:	28.8	5.74	8.16	18.7

A molecular weight determination was also performed by Galbraith Laboratories on  $\text{Eu}(\text{DMAC})_3\text{Cl}_3$ , and the result obtained was approximately half the theoretical molecular weight for  $\text{Eu}(\text{DMAC})_3\text{Cl}_3$ . To perform the analysis, they dissolved the crystals in dimethylformamide (DMF) and measured the lowering of the vapor pressure, a phenomenon associated with the number of particles in solution. Due to the great similarity of the chemistry of DMAC to DMF, no significant measured molecular weight difference is expected between these two solvents. Since the observed molecular weight is one-half

the formula weight, it is concluded that the molecule must dissociate into two particles. There is only one likely dissociation mechanism which yields two distinctly different molecular entities when one molecule of the rare-earth-DMAC complex is dissolved in DMAC. This is indicated by the following equation:



Further dissociation of the complex, in DMAC solution, would produce more  $\text{Cl}^-$  ions which would act as separate particles and produce an apparent molecular weight less than one-half the molecular formula.

If one examines the UV and visible absorption spectra of these complexes dissolved in DMAC, run versus a pure DMAC blank, a strong UV absorption attributable only to the complex is present. This absorption is shifted some 400 Å toward the visible from the usual UV absorption of pure DMAC, which indicates at least a partial delocalization of the DMAC carbonyl electrons.

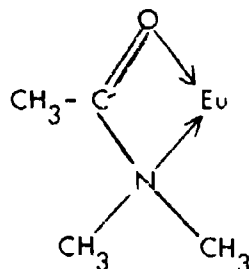
Also, the IR absorption spectrum of the complex in solution shows a shoulder on the carbonyl-stretch band not present in the pure solvent. This can be attributed to a lowering of the carbonyl-stretch frequency within the complex by some  $40\text{ cm}^{-1}$ . The conclusion is that the DMAC is coordinated to the rare-earth ion through the carbonyl oxygen.

The results described above indicate that in the crystalline form, the DMAC complexes are composed of three DMAC molecules and three chloride ions for each rare earth ion, and in solution one of the chloride ions is free, leaving the ion  $\text{M(DMAC)}_3\text{Cl}_2^+$ .

On an investigation of certain homologs of dimethylacetamide, to be discussed in a subsequent section, it was found that when a hydrogen atom is bonded to the nitrogen of the amide group, phosphorescence is severely quenched. This indicates that the nitrogen is also coordinated to the rare-earth ion, for only an N-H bond immediately adjacent to the rare-earth ion is considered to be capable of influencing the phosphorescence to such



an extent. It was therefore concluded that DMAC is acting as a bidentate; that is, coordinating through both oxygen and nitrogen.



DMAC Coordinated to Europium

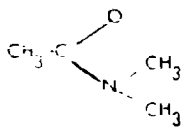
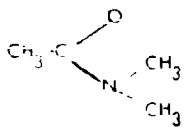
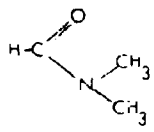
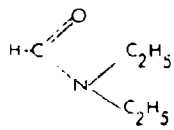
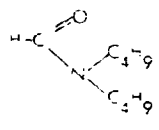
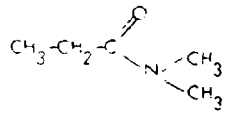
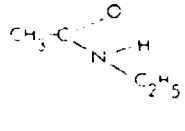
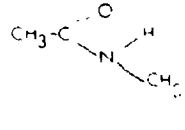
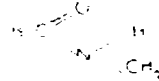
This result was not totally unexpected since coordination numbers of eight or nine (counting the chlorines) are fairly common for rare-earth ions. As relates to the potential of developing a liquid laser, this fact that the ligand behaves as a bidentate has little effect. It does mean, however, that substituents which affect either the carbon-oxygen or the carbon-nitrogen bond may influence the rare-earth phosphorescence, and that the DMAC system is more complicated than was originally anticipated.

#### b. Phosphorescence of Complexes of $\text{Eu}^{+3}$ with Dimethylacetamide and its Homologs

The phosphorescence intensity of each complex with europium is noted in Table 7 for both the 619 nm and 595 nm line (which have different terminal levels, as shown by Figure 1), as well as the ratio of intensity of the 619 nm line to the 595 nm. All measurements were made on the hydrated salts dissolved in excess solvent.

Several things can be noted from Table 7. For the first two complexes listed, the difference is not in the ligand but in the anion. The chloride complex has significantly weaker intensity than its nitrate analog. This indicates the anion plays a role in influencing the phosphorescence of the rare-earth ion. This means that the anions are at least partially within the coordination sphere of the rare-earth ion in solution, and hence bonded to it.

TABLE 2  
Phosphorescence Intensities of DMAC and Its Homologs with Europium (III)

Complex	Ligand	Intensity		$\log I_{595}/I_{619}$
		619 nm	595 nm	
Eu-Cl-Dimethylacetamide		104	20.3	5.14
Eu-Cl-Dimethylacetamide		40.6	12.2	3.33
Eu-H-Dimethylformamide		82.5	18.9	4.36
Eu-N-Diethylformamide		88.1	18.3	4.81
Eu-N-Dibutylformamide		77.3	14.8	5.22
Eu-Cl-Diethylacetamide		94.0	14.3	6.56
Eu-Cl-Ethylacetamide		9.16	3.05	3.01
Eu-Cl-Methylacetamide		3.19	1.10	2.90
Eu-Cl-Methylformamide		< 1.0	< 1.0	--

A nitrate ion has a vibration at  $1380\text{ cm}^{-1}$  whereas, of course, a chloride ion has no internal molecular vibrations at all. Thus, it appears that the nitrate vibration is enhancing the phosphorescence and may be assisting the nonradiative transitions to the emitting level to a greater extent than from the emitting level.

Looking further at the table, there is definite evidence that complexes with monosubstituted amide ligands, that is, those with a hydrogen atom on the nitrogen, yield far weaker phosphorescence than complexes having di-substituted ligands. This is consistent with the idea that a hydrogen bond adjacent to the metal ion provides an excellent mechanism for quenching phosphorescence. If we compare the nitrates of dimethylacetamide and dimethylformamide, we note that the hydrogen on the carbon seems to quench the phosphorescence more than a methyl group, but nowhere as much as a hydrogen on nitrogen. It should be noted, however, that the numbers given are probably good to only 5%, and small differences should not be considered significant.

From the above investigation of DMAC homologues, one can see that molecular changes consisting of adding on varying numbers of  $-\text{CH}_2-$  groups to the DMAC molecule result in only negligible alterations in phosphorescence properties.

#### c. Phosphorescence of the $\text{Tb}^{+3}$ - Dimethylacetamide Complex

As is already well known, water has a strong quenching effect on rare-earth phosphorescence, so that one might suppose that any DMAC solution of a hydrated salt would display a weak output. Therefore experiments were performed to compare the phosphorescence and hydrated rare-earth salts in DMAC. It was found that the solubility in DMAC of hydrated salts (salts containing water of crystallization) far exceeds that of the corresponding anhydrous salts. This is presumably because at least one water molecule remains solvated to the rare-earth ion in the organic liquid, thereby creating an environment more closely approximating that of an aqueous solution in which the salts display great solubility.

It was found that the actual phosphorescence intensity of a 0.44M solution of  $\text{Tb}(\text{NO}_3)_3 \cdot 6\text{H}_2\text{O}$  in DMAC is about thirteen times brighter than a saturated anhydrous  $\text{TbCl}_3$ -DMAC solution (Table 8) which is approximately 0.02M. These figures show that intensity per terbium atom in the solution of the hydrated salt is only about 60% of that in the anhydrous system. However this intensity decrease per atom is more than offset by the much larger number of terbium atoms per cc, so that the total phosphorescence intensity from the solution is greatly enhanced. An interesting conclusion to be drawn from these observations is that the presence of approximately one water molecule per solvation sphere around the Tb causes far less quenching than the case of a complete  $\text{H}_2\text{O}$  solvation sphere which obtains in water solutions of Tb salts. Further experiments showed that dilution of the 0.44M solution with DMAC resulted in a phosphorescence intensity decrease which was directly proportional to the dilution factor. This constancy of emission intensity per Tb ion indicates that no significant self-quenching of the terbium (through Tb-Tb interactions) had been occurring in the concentrated solution, provided one may assume an unvarying constitution of the solvation sphere as more DMAC is added. Evidence for the latter point is the lack of change in the structure of the spectrum accompanying this dilution.

TABLE 8  
Relative Phosphorescent Intensities of Neodymium and  
Terbium in Different Solvents

Concentration	Liquid	Relative Intensities (1)	
~ 0.02 M (Sat)	$\text{TbCl}_3$ -DMAC Anhydrous	5 (5477Å)	5 (4875Å)
0.44 M (~ Sat)	$\text{Tb}(\text{NO}_3)_3 \cdot 6\text{H}_2\text{O}$ -DMAC	65 (5433Å)	65 (4888Å)
0.10 M (~ Sat)	$\text{NdCl}_3$ -DMAC Anhydrous	1.0 (1.06μ)	
1.0 M	$\text{Nd}(\text{NO}_3)_3 \cdot 6\text{H}_2\text{O}$ -DMAC	Undetectable (1.06μ)	

(1) All intensities have been corrected for the known response characteristics of the 7102 photomultiplier and the xenon excitation lamp.

d. Phosphorescent Fine Structure of Complexes of  $Tb^{+3}$  and  $Eu^{+3}$  with Dimethylacetamide

Another technique, aside from conductivity measurements for establishing the existence of more than one molecular species in solution, is the study of the splitting of the phosphorescence bands into a multiplet structure; each component arising from some particular entity. A Jarrell-Ash 0.5 meter Ebert scanning monochromator was set up in conjunction with a 150 watt xenon excitation lamp and an 1P21 photomultiplier tube feeding a recorder through an amplifier. Suitable filtering of the exciting light was used in order to completely remove the europium and terbium phosphorescence wavelength regions, so as to minimize any interference. Another filter removed the infra-red to prevent the heating of the sample. This monochromator has a dispersion of 16Å per mm and was used with a 30  $\mu$  output slit giving an actual resolution capability of 0.48Å.

With this experimental set-up, solutions of anhydrous and hydrated europium and terbium salts in DMAC were examined for resolvable fine structure in their phosphorescence spectra. A saturated anhydrous  $TbCl_3$  solution in DMAC yielded spectra where the  $^5D_4 \rightarrow ^7F_6$  (approximately 490 m $\mu$ ) phosphorescence transitions were split into doublets (Table 9).

In an attempt to establish the origin of these doublets, two drops of water were added to 3cc of the anhydrous solution. This resulted in the disappearance of one of the components from each of the doublets, and a considerable overall decrease in the phosphorescence intensity from both of the transitions. The frequency of the remaining lines are very close to those from both an aqueous solution of  $TbCl_3$  and a DMAC solution of  $Tb(NO_3)_3 \cdot 6H_2O$ .

Due to the complexity of the systems it is not possible to determine unambiguously what molecular changes are responsible for the above result, although two explanations came to mind as being reasonable. The supposed anhydrous solution may not be strictly dry and may contain a small amount of water. If there was not enough water to contribute at least one molecule to the first solvation sphere of all the terbium ions, then two molecular species would exist; some possessing at least one water about the terbium

and others none. The two species would then have different rare-earth environments and could give rise to phosphorescence spectra at somewhat different frequencies. Adding more water would assure that all of the terbium ions have at least one water in close proximity and the spectra from the species with no water could, of course, disappear. The decreased phosphorescence intensity would then result from the well known quenching effect of water.

Alternatively, the anhydrous system may be strictly dry and the splitting may result from the lifting of the degeneracies of the emitting and terminal levels by a strong electric field of a particular symmetry resulting from the coordination sphere around the terbium. The addition of water can now create an environment of different symmetry which does not split the degenerate terbium levels into as many components as before, so that only one band is observed.

As can be seen from Table 9 the europium nitrate and chloride-DMAC and water solutions do not display any splitting of the phosphorescence bands, although a close examination of the band shape reveals some asymmetry which is indicative of the possible presence of unresolved overlapping components. It is not yet clear why the europium and terbium systems behave in such a different manner. However, the Eu levels have smaller J-values than the Tb levels, and so might display a lesser spread of local field components.

#### e. Phosphorescence of the $\text{Nd}^{3+}$ -Dimethylacetamide Complex

A 0.1M solution (practically saturated) of anhydrous  $\text{NdCl}_3$  in DMAC displayed a weak phosphorescence at  $1.06\mu$  as compared with the intensity in the green from the corresponding anhydrous terbium system. From Table 8 we see that per neodymium atom the intensity is approximately 0.04 times that of the per-atom terbium intensity.

Although the Nd salt containing water of crystallization,  $\text{Nd}(\text{NO}_3)_3 \cdot 6\text{H}_2\text{O}$ , was soluble to the extent of 1.0 M in DMAC, no  $1.06\mu$  phosphorescence could be detected at all, in strong contrast to the situation for the Tb case. This indicates the extreme sensitivity of neodymium phosphorescence to the proximity of water molecules to the neodymium atom, since at least one water molecule is present in the immediate solvation sphere of the rare-earth.

TABLE 9

Phosphorescent Fine Structure of Europium and Terbium in DMAC and Water Systems

	Wavelength in Å of Center of Phosphorescence Peaks
$\text{Tb}(\text{NO}_3)_3 \cdot 6\text{H}_2\text{O}-\text{DMAC}$	5433 4888
$\text{TbCl}_3-\text{H}_2\text{O}$	5430 4884
$\text{TbCl}-\text{DMAC}$ Anhydrous	5477 } 5423 } 4952 } 4875 }
$\text{TbCl}_3-\text{DMAC}$ Anhydrous	5435
plus small amount of water	4878
$\text{EuCl}_3-\text{DMAC}$ Anhydrous	6115 5910
$\text{EuCl}_3-\text{DMAC}$ Anhydrous	6115
plus small amount of water	5910
$\text{EuCl}_3-\text{H}_2\text{O}$	6119 5910
$\text{Eu}(\text{NO}_3)_3 \cdot 6\text{H}_2\text{O}-\text{DMAC}$	6166 5985

In the light of our ideas which view non-radiative transitions as arising from transfer of the electronic energy of the rare-earth atom to vibrational modes of groups in close proximity, we can rationalize the above difference between Nd and Tb behavior. The efficiency of energy transfer progressively falls as the bond which is being vibrationally excited is moved further from the rare-earth. Also, if one has to excite a high vibrational overtone to accept the energy then the transfer is very much less efficient than if the transfer can be accomplished by excitation of a low overtone. Since the energy gap in Nd between the emitting level ( ${}^4F_{3/2}$ ) and the next lowest level ( ${}^4I_{15/2}$ ) is only  $5500\text{ cm}^{-1}$ , one can readily see that for C-H and O-H stretching vibrations, which are usually broad bands from  $3000$  to  $3500\text{ cm}^{-1}$ , a vibrational excitation to the second overtone ( $v=2$  level) will suffice. In terbium the similar energy gap is approximately three times as many wavenumbers so that non-radiative energy transfer, which must now involve high frequency vibrations, is very much less efficient.

Thus, even though the C-H stretching vibration present in DMA is removed from the immediate vicinity of the neodymium (which is coordinated through the oxygen and nitrogen), it is still very effective in promoting non-radiative relaxations among the closely spaced energy levels of that ion. It appears, therefore, that in order to obtain really strong  $1.06\mu$  neodymium phosphorescence, one would have to completely remove all high frequency vibrations from the solvation sphere of the ion.

##### 5. Criteria for Pumping Europium Systems

In any potential laser material relying on optical pumping, it is necessary to consider the power level of the optical pump needed to obtain laser action. Basically the optical pump must generate enough useful power, as a pulse or continuously, so that the critical population inversion is developed in the laser material. In either mode of excitation, the power level for a three-state laser is in part determined by the observed phosphorescence lifetime and the quantum efficiency. Given two  $\text{Eu}^{+3}$  systems which are energetically identical, the one with a longer observed phosphorescence lifetime and a higher quantum efficiency will have a lower power threshold for laser action.



Even though the  $\text{Eu}^{+3}$  phosphorescence can be schematically represented as a four level laser, the room temperature populations of  ${}^7\text{F}_1$  and  ${}^7\text{F}_2$  are sufficiently high so that the threshold power requirements are essentially those of a three level laser.

The observed lifetime  $T$  of an excited state can be defined by the following expression:

$$\frac{1}{T} = \frac{1}{t_r} + \frac{1}{t_n} \quad (5-1)$$

where  $t_r$  and  $t_n$  are the radiative and non-radiative lifetimes, respectively. The radiative lifetime of a transition can be quite long if the spontaneous transition probability is low, as in the case with rare-earth phosphorescence. It is seen that the observed lifetime is a harmonic combination of the two relaxation mechanisms; hence, by reducing the non-radiative relaxation contribution, the observed lifetime can be increased to the limit where it equals the radiative lifetime. Such a case where the observed lifetime equals the radiative lifetime is said to have a radiative quantum efficiency of 1.0. (The radiative quantum efficiency must be distinguished from the overall quantum efficiency, which includes losses incurred before the radiating state is reached.) Threshold power levels can be calculated by considering the kinetics of the overall phosphorescence.

Let us start with the  $4f^6$  energy level diagram for  $\text{Eu}^{+3}$  in Figure 17 with the indicated transition probabilities.  $W_{15}$  is the optically-induced transition probability from the ground state ( ${}^7\text{F}_0$ ) to some metastable state ( $M_i$ ) and depends upon the absorption coefficient of the transition as well as the power level of the pumping radiation. The excitation rate or the number of atoms excited into  $M_i$  per second is given by  $W_{15}N_1$ . The state  $M_i$  is representative of any one of the several intermediate states which can be produced by exciting with each of the absorption bands of the  $\text{Eu}^{+3}$  complex.

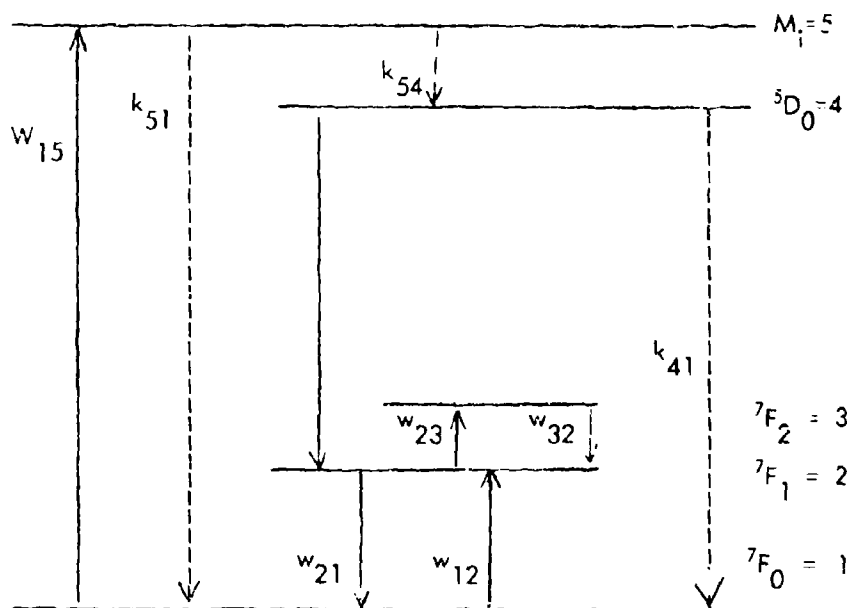


FIGURE 17

Energy Level Diagram for  $\text{Eu}^{+3}$ 

The thermally-induced transition probabilities  $w_{32}$ ,  $w_{23}$ ,  $w_{21}$ , and  $w_{12}$  correspond to the transitions  $^7F_2 \rightarrow ^7F_1$  and  $^7F_1 \rightarrow ^7F_0$ . The spontaneous processes which relax the  $^5D_0$  states are the radiative phosphorescence transitions  $^5D_0 \rightarrow ^7F_2$  ( $k_{43}$ ) and  $^5D_0 \rightarrow ^7F_1$  ( $k_{42}$ ) and all the non-radiative processes are collectively represented by  $k_{41}$  so that the observed lifetime  $T$  of the emitting level is given by:

$$\frac{1}{T} = k' = k_{42} + k_{43} + k_{41} \quad (5-2)$$

The overall quantum efficiency of a phosphorescent material is defined as the number of quanta emitted per quantum absorbed. This term serves to monitor the non-radiative relaxation of  $M_i$  to the emitting  ${}^5D_0$  state and the subsequent radiative transition to the ground state (see Figure 16).

The  $M_i$  relaxation mechanism can be broken up into three processes: (1) the non-radiative relaxation  $M_i \longrightarrow {}^5D_0$ , (2) the radiative relaxation  ${}^5D_0 \longrightarrow {}^7F_1$  or  ${}^7F_2$ , (3) the non-radiative relaxation  ${}^5D_0 \longrightarrow {}^7F_0$ . The overall quantum efficiency of the  ${}^5D_0$  state is then:

$$n = n' \left( \frac{k_r}{k_r + k_{41}} \right) \quad (5-3)$$

where  $n'$  is the number of  ${}^5D_0$  states generated per  $M_i$  state,  $k_r$  is the radiative transition probability for  ${}^5D_0 \longrightarrow {}^7F_1$  and  ${}^7F_2$  and  $k_{41}$  is the non-radiative transition probability for  ${}^5D_0 \longrightarrow {}^7F_0$ .

Or in terms of the relaxation times

$$n = n' \left( \frac{t_r}{t_r + t_n} \right) \quad (5-4)$$

where  $t_n$  = non-radiative lifetime

$t_r$  = radiative lifetime of  ${}^5D_0$

(The radiative quantum efficiency is given by  $n/n'$ ).

It is seen from Figure 17 that:

$$n' = \frac{k_{54}}{k_{51} + k_{54}} \quad (5-5)$$

From the above analysis, the overall quantum efficiency is determined by two processes: the non-radiative relaxation  $M_1 \longrightarrow {}^7F_0$  and the non-radiative relaxation of  ${}^5D_0$ . For an efficient phosphorescence system we would want to minimize both. The chemical environment about the emitting ion is intimately involved in each of these factors. Both of these processes are considered to be related to the vibrational degrees of freedom of the ligand field in the immediate vicinity of the emitting ion. It is thought that the non-radiative relaxation mechanism proceeds through a coupling of the phosphorescent electronic energy levels with overtones of the vibrational degrees of freedom of neighboring bonds. The probability for non-radiative relaxation decreases as the quantum number of the overtone increases. The quantum efficiency of the  $\text{Eu}^{+3}$  phosphorescence can then be increased by coordinating the rare earth ion with groups whose vibrational energy is toward the long wavelength region of the infrared.

#### 6. Power Threshold Calculation for Europium Systems

If we assume the existence of a steady state, the scheme in Figure 17 leads to the following rate equations:

$$\begin{aligned}
 \frac{dN_5}{dt} &= W_{15}N_1 - N_5k_{54} - N_5k_{51} = 0 \\
 \frac{dN_4}{dt} &= N_5k_{54} - N_4(k_{43} + k_{42} + k_{41}) = 0 \\
 \frac{dN_3}{dt} &= N_4k_{43} + N_2w_{23} - N_3w_{32} = 0 \\
 \frac{dN_2}{dt} &= N_4k_{42} + N_3w_{32} + N_1w_{12} - N_2(w_{23} + w_{21}) = 0 \\
 \frac{dN_1}{dt} &= N_4k_{41} + N_2w_{21} - N_1(W_{15} + w_{12}) = N_5k_{51} = 0 \\
 \text{and } N_0 &= \sum_{i=1}^5 N_i
 \end{aligned} \tag{6-1}$$

where  $N_i$  is the population of the  $i$ -th energy level and  $N_0$  is the concentration of  $\text{Eu}^{+3}$  in atoms/cc. From the quantum efficiency measurement we have shown that:

$$k_{54} \geq k_{51}$$

Without loss of generality we can assume that all the lost excited states degrade via  $k_{51}$  and that  $k_{41} = 0$ . Then  $k_{54} = k_{51}$ . This is the most unfavorable case.

The transition of interest for these  $\text{Eu}^{+3}$  complexes is  ${}^5\text{D}_0 \rightarrow {}^7\text{F}_2$ . Therefore, it is necessary to calculate at what excitation rate ( $N_1 W_{15}$ ) will  $N_4$  be greater than  $N_3$  to such an extent as to sustain laser action in a cavity of known dimensions. Solving the above series of equations for the steady-state ratio of  $\frac{N_4}{N_3}$  we get:

$$\frac{N_4}{N_3} = \frac{W_{15}}{2k'} \cdot \frac{g_1}{g_3} \cdot \exp \left[ -(E_3 - E_1)/k\theta \right] \quad (6-2)$$

( $\theta$  = absolute temperature)

where  $k'$  is given by Equation (5-2) and  $g_1$  and  $g_3$  are the degeneracies of the  ${}^7\text{F}_0$  and  ${}^7\text{F}_2$  energy levels, respectively. In deriving Equation (6-2), we have recognized that  $k'$  is primarily radiative and that the thermally-induced transition probabilities  $w_{ij}$  are much greater than  $W_{15}$ . As a result, the transition probability ratios for  ${}^7\text{F}$  states will approach the equilibrium distribution ratios, which are given by the exponential and the multiplicity ratio in Equation (6-2). Rewriting Equation (6-2) so that the two levels are equally populated, we get:

$$\frac{1}{2} (N_1 W_{15}) = \frac{g_3}{g_1} \cdot \exp \left[ -(E_3 - E_1)/k\theta \right] \quad (6-3)$$

By multiplying both sides of Equation (8-3) by  $N_1$  we get:

$$\frac{1}{2} (N_1 W_{15}) = \frac{N_1 g_3}{g_1} \cdot \exp \left[ -(E_3 - E_1)/k\theta \right] \quad (6-4)$$

The right side is  $N_3$ , the steady state population of the  ${}^7F_2$  state, so that:

$$W_{15}N_1 = \frac{2N_3}{T} \quad (6-5)$$

This equation serves to contrast three- and four-level lasers. If  $E_3$  is sufficiently above  $E_1$ , say  $(E_3 - E_1) > 8k\theta$ , then levels 4 and 3 are equally populated before any pumping, i.e. both  $N_4$  and  $N_3$  are effectively zero. However, if  $N_3$  is not initially zero, as in the case of  $\text{Eu}^{+3}$  ( $E_3 - E_1 \approx 5k\theta$ ), a modified three-level laser results, for which an initial amount of pump flux, given by Equation (6-5), is first required to equalize the population of the  ${}^5D_0$  and  ${}^7F_2$  states.

For a typical case, take an 0.02 M solution of  $\text{EuCl}_3 \cdot 3\text{HMPA}$  in HMPA with a measured lifetime of  $\sim 1$  msec; the excitation rate per cc of solution for equalization is  $5.60 \times 10^{20}$  atoms/sec at a particular absorption band. In this calculation we have taken the initial populations of the  ${}^7F_0$  and  ${}^7F_2$  states as approximating the steady state values of  $N_1$  and  $N_3$ . However, in order to obtain laser action a certain critical excess of population in the upper state  $(N_4 - N_3)_c$  must be developed. According to laser theory the critical inversion  $(N_4 - N_3)_c$  that is required to sustain laser action in the cavity of certain length is given by:

$$(N_4 - N_3)_c = \frac{4\pi^2\nu^2\Delta\nu t}{c^3 \cdot t_c} \quad (6-6)$$

where  $\nu$  = fluorescence line frequency

$\Delta\nu$  = line width

$t$  = radiative lifetime

$t_c$  = cavity lifetime (related to all the cavity loss mechanisms)

$c$  = velocity of light in the medium.

Upon substitution into Equation (6-6) a value of  $7.6 \times 10^{17}$  atoms/cc is obtained for the critical inversion so that the steady state excitation rate per cc of solution is  $2.08 \times 10^{21}$  atoms/sec.

In this calculation we have used the emission line at 619 nm with a line width of 20 Å as the laser wavelength and assumed that the loss per pass in a cavity of length 5 cm is 10%.

The pump power level at the excitation wavelengths necessary to excite  $2.08 \times 10^{21}$  atoms/sec-cc depends upon the absorption spectrum of the  $\text{Eu}^{+3}$  complex. The absorption spectrum of the  $\text{Eu}^{+3}$  complexes between 350 nm to 600 nm reveals several absorption bands including two moderate ones at 395 nm and 465 nm with extinction coefficients of about 1.5 and 1.0, respectively. Since the absorption at 395 nm and 465 nm is relatively small, a calculation of the pump power level based on one pass through the laser material is wasteful. However, if the cavity is constructed so that an unlimited number of efficient passes is possible, effectively all of the pump radiation at the absorption band can be absorbed. This mode of excitation is advantageous since it affords a homogeneous excitation throughout the laser medium. Therefore, if the output of the optical pump is  $P^0(\lambda)$  quanta per sec per unit wavelength, or  $\frac{P'(\lambda)}{N}$  where  $P'(\lambda)$  is the pumping power in watts per unit wavelength, and considering only the 395 nm and 465 nm absorption bands, the following equation established the pumping level:

$$\frac{c}{h} [P_1 \cdot \lambda_1 + P_2 \cdot \lambda_2] \Delta\lambda = N_1 W_{15} \quad (6-7)$$

where  $\Delta\lambda$  = the line width ( $\Delta\lambda_1 = \Delta\lambda_2$ ).

The indices (1) and (2) refer to the two absorption bands at which excitation occurs. Assuming that the power level is constant over the wavelength range of interest, and using the measured line width of 50 Å for each absorption band, Equation (6-7) yields:

$$P' = 6.30 \text{ watt-cc per Angstrom interval} \\ \text{of the lamp output spectrum.}$$

TABLE 10  
Relative Phosphorescent Intensities of Terbium Lines\*

Complex	$^5D_4 \rightarrow ^7F_4$ (625 nm)	$^5D_4 \rightarrow ^7F_4$ (587 nm)	$^5D_4 \rightarrow ^7F_5$ (548 nm)
Tb-N-DMSO		0.25 0.23 0.27 0.18 <u>0.23</u> Ave.	2.06 1.57 1.60 1.34 <u>1.67</u> Ave
Tb-Cl-DMSO		0.25	1.98
Tb-N-DMAC	0.019	0.19 0.16 0.14 0.13 <u>0.15</u> Ave.	2.22 2.16 2.05 1.27 <u>1.93</u> Ave.
Tb-Cl-DMAC		0.13	2.16
Tb-N-DMF		0.18 0.17 0.18 <u>0.18</u> Ave.	2.24 2.00 1.99 <u>2.08</u> Ave.
Tb-Cl-DMF	0.012	0.18	2.70
Tb-N-TEP	0.007	0.16 0.15 0.16 0.15 <u>0.16</u> Ave.	2.27 2.18 2.12 1.90 <u>2.12</u> Ave.
Tb-N-TRP		0.17 0.15 <u>0.16</u> Ave.	2.16 1.93 <u>2.05</u> Ave.
Tb-N-H <sub>2</sub> O		0.22 0.20 0.28 0.23 <u>0.23</u> Ave.	1.49 1.41 1.63 1.63 <u>1.45</u> Ave.

\* The intensity of the  $^5D_4 \rightarrow ^7F_6$  line (487 nm) is taken as unity; it is therefore not listed



### 7. Phosphorescent Intensities and Lifetimes of $Tb^{+3}$ Complexes

A number of phosphorescent spectra of terbium complexes have been taken. Table 10 shows the uncorrected relative intensities of the lines at 487, 548, 587 and 625 nm. The peak areas (height x full width at half height) are normalized on the 487 nm line. The  $^5D_4 \rightarrow ^7F_5$  (625 nm) line is quite weak, and the few values given were obtained from spectra run at greater sensitivity in which only the 625 nm and 586 nm lines were measured. These should be considered as "order of magnitude" values.

The lifetimes of several  $Tb^{+3}$  complexes were measured and are listed in Table 11. Also listed are the coordinating groups with their respective fundamental stretching frequencies.

TABLE 11  
Lifetimes of Various  $Tb^{+3}$  Complexes

Complex	Lifetime (Milliseconds)	Stretching frequency of coordinating group ( $cm^{-1}$ )
$Tb(NO_3)_3$ in dimethyl sulfoxide	$2.40 \pm 0.20$	1030
$Tb(NO_3)_3$ in triethyl phosphate	$2.45 \pm 0.18$	1200
$Tb(NO_3)_3$ in tri-n-butyl phosphate	$2.25 \pm 0.35$	1200
$Tb(NO_3)_3$ in dimethyl formamide	$1.58 \pm 0.06$	1600
$Tb(NO_3)_3$ in dimethyl acetamide	$1.62 \pm 0.06$	1600
$Tb(DBP)_3$ (solid) (DBP = $(C_4H_9O)_2PO_2$ )	$9.09 \pm 0.63$	1200

Unlike  $Eu^{+3}$ , we can excite, with a high degree of efficiency, directly into the emitting level of  $Tb^{+3}$  from the ground state. This affords an opportunity to determine the absolute non-radiative efficiency  $\eta$  and directly compare the quantum yields at different excitation wavelengths.

The  $\text{Tb}^{+3}$  fluorescence is due primarily to transitions from the  $^5\text{D}_4$  excited state to several of the  $^7\text{F}$  ground multiplets as indicated in Figure 18. The lifetime is then:

$$\tau = \frac{1}{k_0 + k_3 + k_4 + k_5 + k_6}$$

where  $k_i$  is the appropriate rate constant for the transition to the  $i^{\text{th}}$  terminal state and  $k_0$  is the non-radiative relaxation rate constant.

The non-radiative  $^5\text{D}_4 \rightarrow ^7\text{F}_0$  relaxation is considered to be the principal mechanism for energy dissipation of the  $^5\text{D}_4$  excited state. The energy difference between the  $^5\text{D}_4$  and  $^7\text{F}_0$  states is  $14,400 \text{ cm}^{-1}$  so that we can expect the non-radiative relaxation rate constant  $k_0$  to be comparable to  $k_3$  ( $^5\text{D}_0 \rightarrow ^7\text{F}_3$ , energy interval  $12,000 \text{ cm}^{-1}$ ) of  $\text{Eu}^{+3}$ . Based on a calculation of  $k_6$  from the absorption coefficient of the  $^7\text{F}_6 \rightarrow ^5\text{D}_4$  transition, it has been found that the radiative rate constants for the  $\text{Tb}^{+3}$  phosphorescence are comparable to  $k_1$  ( $^5\text{D}_0 \rightarrow ^7\text{F}_1$  transition) of  $\text{Eu}^{+3}$ . This means that the radiative lifetime of a  $\text{Tb}^{+3}$  complex will generally be longer than that of the corresponding  $\text{Eu}^{+3}$  complex. This is due to the presence in the  $\text{Eu}^{+3}$  phosphorescence of the  $^5\text{D}_0 \rightarrow ^7\text{F}_2$  transition whose radiative lifetime is usually much less than that of  $^5\text{D}_0 \rightarrow ^7\text{F}_1$ . The longer radiative lifetime of the  $\text{Tb}^{+3}$  phosphorescence should result in a lower radiative efficiency than that of the corresponding  $\text{Eu}^{+3}$  complex.

The absorption data for the  $^7\text{F}_6 \rightarrow ^5\text{D}_4$  transition are preliminary, but they indicate that  $k_6$  does not vary more than 20% in each of the soluble complexes listed in Table 10. Since we have previously found that the relative intensity distribution of the  $\text{Tb}^{+3}$  emission bands is nearly the same for each complex, we conclude that the rate constants  $k_3$ ,  $k_4$  and  $k_5$  are also invariant. Therefore, we have

$$k_6 + k_5 + k_4 + k_3 = k \approx \text{const.}$$

and the lifetime becomes

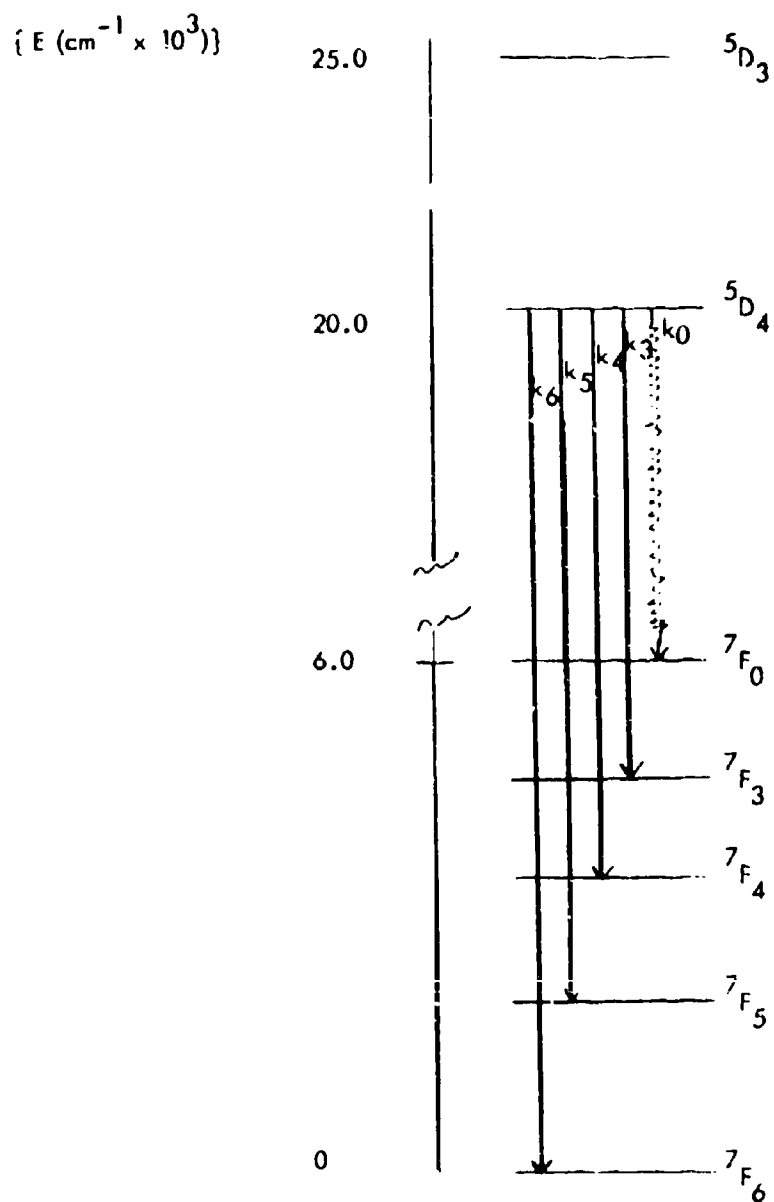
$$\tau = \frac{1}{k_0 + k}$$

This indicates that the  $Tb^{+3}$  lifetime should only be affected by changes in the non-radiative relaxation rate constant  $k_0$ . Therefore, for a given vibrational environment, the  $Tb^{+3}$  lifetime is expected to be constant.

The lifetimes listed in Table 10 bear out this point. It is seen that for a particular vibrational environment the observed lifetime is essentially constant. The short lifetime of the DMF and DMAC complexes is due to the relatively high C-O stretching frequency which contributes more effectively to the non-radiative relaxation. The long lifetime of the  $Tb(DBP)_3$  is presumably due to the elimination of the  $NO_3^-$  ion from the ligand environment. If the  $NO_3^-$  ion does contribute significantly to the non-radiative relaxation as indicated, then the  $TbCl_3$  complexes should have longer lifetimes than those listed in Table 10. The lifetimes of the  $TbCl_3$  complexes should be determined and compared to their  $NO_3^-$  ion analogues.

If we consider the implications of these data for a potential terbium liquid laser, we can draw the following tentative conclusions:

1. The most promising laser transition is  $^5D_4 \longrightarrow ^7F_5$  which is the most intense in all cases. The terminal state is about  $2300\text{ cm}^{-1}$  above ground level so that this can be a four-state laser to good approximation.
2. The most promising complex would be one which combines high relative intensity of this line with long fluorescent lifetime (minimal non-radiative relaxation). The phosphate and amide complexes are superior in the first particular, the phosphate and sulfoxide complexes in the second. It therefore appears that for terbium, as for europium, the alkyl phosphate complexes are most promising for laser applications.



$4f^8$  ENERGY LEVEL DIAGRAM FOR  $Tb^{+3}$

FIGURE 18

8. Phosphorescence of Complexes of Samarium(III) and Dysprosium(III) with Triethyl Phosphate

The phosphorescence of  $\text{Sm}^{+3}$  and  $\text{Dy}^{+3}$  was measured in  $\text{H}_2\text{O}$  and in TEP. We found that the phosphorescence of both ions is significantly enhanced in TEP. The phosphorescence of  $\text{DyCl}_3$  in both  $\text{H}_2\text{O}$  and TEP is one line at about 580 nm so that the reduction of the non-radiative transfer cannot be separated from any change of the radiative rate constant by the comparison of line intensity ratios. However, the  $\text{Sm}^{+3}$  emission is composed of three lines at about 560, 592 and 650 nm which all originate from the same level. The TEP emission indicates that a radiative enhancement of the 560 nm and 650 nm bands relative to the 592 nm has occurred, as well as a decrease of the non-radiative relaxation rate. These results are still preliminary and further work should be undertaken in this area.

## III. RECOMMENDATIONS

A variety of systems, including the solution of rare-earth salts in organic and inorganic solvent media, have already been examined on this program. Many important properties including phosphorescent intensities and phosphorescent lifetimes have been measured. Other equally significant properties such as solubilities, stabilities and viscosities have also been noted. From these studies, several interesting concepts relating chemical structure and composition to phosphorescent properties have been advanced and several systems selected for more intensive investigations. As a direct result of this work, a very highly promising liquid laser system, neodymium oxide dissolved in a mixture of phosphorus oxychloride and tin tetrachloride, has been developed. Although several other liquid systems have been developed by others while this program was in progress, none appear as promising as the  $\text{POCl}_3\text{-SnCl}_4$  system. This advancement in the state-of-the-art was a direct result of the work in liquid parameters. Considerable more work remains to be done to more completely characterize these parameters and to develop the  $\text{Nd(III) - POCl}_3\text{-SnCl}_4$  system to its full potential.

# REFERENCES

1. General Precision, Inc., Interim Reports on Liquid Laser Parameters, Contract Nonr-4644(00).
2. R. P. Borkowski, H. Forest and D. Grafstein, J. Chem. Phys., **42**, 2974 (1965).
3. H. Forest, A. Samuel and D. Grafstein, J. Opt. Soc. Amer., **56**, 548 (1966).
4. N. Blumenthal, C. Ellis and D. Grafstein, J. Chem. Phys., **48**, 5726 (1968).
5. A. Heller, Appl. Phys. Lett., **9**, 106 (1966).
6. E. J. Schimitschek, Appl. Phys. Lett., **3**, 117 (1963).
7. A. Lempicki and H. Samelson, Phys. Lett., **4**, 133 (1963).
8. S. Bjorklund, C. Kellermeyer, C. Hunt, N. McAvoy and N. Filipescur, Appl. Phys. Lett., **10**, 160 (1967).
9. S. Bjorklund, C. Kellermeyer, N. McAvoy and N. Filipescur, J. Sci. Instrum., **44**, 947 (1967).
10. E. Schimitschek, R. Nehrich and J. Trias, Appl. Phys. Lett., **9**, 103 (1966).
11. A. Heller, J. Amer. Chem. Soc., **89**, 167 (1967).
12. E. Smitzer in Quantum Electronics, Proceedings of the Third International Congress, P. Gruet and N. Bloembergen, Ed., Columbia University Press, New York, N.Y. 1964, p. 999.
13. J. Van Wazer, Phosphorus and Its Compounds, Vol. I., Interscience, New York, N. Y., 1958, p. 254.
14. F. Garner and S. Sugden, J. Chem. Soc., 1298 (1929).
15. A. Heller, J. Mol. Spectrosc., **28**, 101 (1968).
16. General Telephone and Electronics Semiannual Technical Summary Report on High-Energy Pulsed Liquid Laser, Contract N00014-68-C-0110, December 31, 1967.
17. J. L. Kropp and M. W. Windsor, J. Chem. Phys., **39**, 2769 (1963).
18. J. J. Freeman, G. A. Crosby and K. E. Lawson, J. Mol. Spectrosc., **13**, 399 (1964).

APPENDIXDETERMINATION OF NEODYMIUM CONCENTRATION IN LASING SOLUTIONS

The concentration of  $\text{Nd}^{+3}$  in lasing solutions was determined by a combination hydrolytic-spectrometric technique. Standard solutions of  $\text{Nd}^{+3}$  were prepared in the following manner. A weighed quantity of neodymium oxide was dissolved in 5 ml of 50% hydrochloric acid. Phosphorus oxychloride (1 ml) and tin tetrachloride (0.2 ml) were carefully added to this solution and the volume adjusted to 50 ml with 50% hydrochloric acid. The visible absorption spectra of these solutions were obtained on a Beckman DK-2A Spectrophotometer in 1 cm diameter cells. The percent absorption of the  $\text{Nd}^{+3}$  band at 570 nm was plotted against concentration of  $\text{Nd}^{+3}$  in solution. A Beer-Lambert relationship was followed in the range  $5.0 \times 10^{-3}$  to  $2.0 \times 10^{-2}$  moles  $\text{Nd}^{+3}$  per liter. Data for this concentration range is listed below.

<u><math>[\text{Nd}^{+3}]</math></u>	<u>Percent Absorption</u>
$5.0 \times 10^{-3}$	7
$6.8 \times 10^{-3}$	9
$1.0 \times 10^{-2}$	13
$2.0 \times 10^{-2}$	24

Samples of lasing solutions were prepared for analysis by taking 1 ml of the solution and carefully hydrolyzing with 50% hydrochloric acid to a volume of 50 ml. The percent absorption of the band at 570 nm was measured, and the concentration of  $\text{Nd}^{+3}$  determined from the plot of percent absorption versus known concentration. The concentration of  $\text{Nd}^{+3}$  in the lasing solution was then calculated in the normal manner.



UNCLASSIFIED

Security Classification

DOCUMENT CONTROL DATA R & D		
(Security classification of title, body of abstract and indexing annotation must be entered when the overall report is classified)		
1. ORIGINATING ACTIVITY (Corporate author) Singer-General Precision, Inc. Aerospace Research Center Materials Department Little Falls, N.J. 07424		2a. REPORT SECURITY CLASSIFICATION UNCLASSIFIED
3. REPORT TITLE  LIQUID LASER PARAMETERS		2b. GROUP
4. DESCRIPTIVE NOTES (Type of report and inclusive dates) FINAL August 1, 1964 - July 31, 1968		
5. AUTHOR(S) (Last name, middle initial, first name) William Block Daniel Grafstein Robert Barnes		
6. REPORT DATE November 25, 1968	7a. TOTAL NO. OF PAGES 71	7b. NO. OF REFS 18
8a. CONTRACT OR GRANT NO. NONR-4644(00)	8b. ORIGINATOR'S REPORT NUMBER(S)	
8c. PROJECT NO. .	8d. OTHER REPORT NO(S) (Any other numbers that may be assigned this report) .	
10. DISTRIBUTION STATEMENT This document has been approved for public release and sale; its distribution is unlimited.		
11. SUPPLEMENTARY NOTES		12. SPONSORING MILITARY ACTIVITY Office of Naval Research Physical Sciences Division Washington, D. C. 20360
13. ABSTRACT This program was designed to study the influence of chemical and physical environmental factors upon the intensity, efficiency, and lifetime of rare earth phosphorescence in liquid systems. The objective of this program was the development of criteria for the selection of optimum coordinating ligands, counter ions and solvents for rare earths so that useful and efficient high power solution lasers could be developed. A large number of rare earth coordination compounds were synthesized and studied both in the solid state and in solution. A considerable amount of useful information was compiled for systems in which lasing could be accomplished through direct optical excitation of the rare earth. It was concluded that light atoms such as hydrogen and deuterium which would contribute to high-energy vibrational frequencies must be removed from the immediate ligand field surrounding the rare earth ion. Vibrational frequencies in the ligand or coordinating solvent should closely match the energy gaps between the initially excited optically pumped level and the emitting level in order to efficiently populate that level by a cascade process. These same vibrational frequencies, however, must be sufficiently different from the frequency of lasing radiation so as not to promote non-radiative transitions from the emitting level. Of the several organic and inorganic solvents that were investigated, those in which a phosphorus-oxygen linkage was coordinated to the		

DD FORM 1473  
1 NOV 65

UNCLASSIFIED

Security Classification

UNCLASSIFIED

Security Classification

Sheet No. 2

DOCUMENT CONTROL DATA R & D		
(Security classification of title, body of abstract and indexing annotation must be entered when the overall report is classified)		
1. ORIGINATING ACTIVITY (Corporate Author)		2a. REPORT SECURITY CLASSIFICATION
LIQUID LASER PARAMETERS		2b. GROUP
3. REPORT TITLE		
4. DESCRIPTIVE NOTES (Type of report and inclusive dates)		
5. AUTHOR(S) (First name, middle initial, last name)		
6. REPORT DATE	7a. TOTAL NO. OF PAGES	7b. NO. OF REFS
8a. CONTRACT OR GRANT NO.	8b. ORIGINATOR'S REPORT NUMBER(S)	
9. PROJECT NO.	9b. OTHER REPORT NO(S) (Any other numbers that may be assigned this report)	
10. DISTRIBUTION STATEMENT		
11. SUPPLEMENTARY NOTES	12. SPONSORING MILITARY ACTIVITY	
13. ABSTRACT (continued)		
<p>rare earth appeared most promising. As a direct result of this work, a very highly promising liquid laser system, neodymium oxide dissolved in a mixture of phosphorus oxychloride and tin tetrachloride, has been developed. The solution is quite stable in a closed system and does not exhibit any visual decomposition phenomenon when subjected to the excitation of a Xenon flash lamp. The neodymium-phosphorus oxychloride-tin tetrachloride laser is one of the most promising liquid lasers yet developed and, when optimized, could lead to an efficient, high power, continuous system.</p>		

DD FORM 1473  
1 NOV 65

UNCLASSIFIED

Security Classification

UNCLASSIFIED

Security Classification

KEY WORDS	LINK A		LINK B		LINK C	
	ROLE	WT	ROLE	WT	ROLE	WT
Liquid Lasers Rare Earth Phosphorescence Neodymium-Phosphorus Oxychloride Tin Tetrachloride Laser						

UNCLASSIFIED

Security Classification